Manuscript submitted to eLife Reviewed Preprints

Guanidine Production by Plant Homoarginine-6-hydroxylases

Dietmar Funck[1]*, Malte Sinn[1], Giuseppe Forlani[2], and Jörg S. Hartig[1]*

[1] Department of Chemistry, University of Konstanz, 78457 Konstanz

[2] Department of Life Science and Biotechnology, University of Ferrara, 44121 Ferrara, Italy

* Correspondence: Jörg S. Hartig, Dietmar Funck

Email: joerg.hartig@uni-konstanz.de, dietmar.funck@uni-konstanz.de

Subject areas: Biochemistry and Chemical Biology, Plant Biology

Keywords: Guanidine, Homoarginine, Fe^{2+}- and 2-oxoglutarate dependent dioxygenase, aldehyde dehydrogenase, *Arabidopsis thaliana*.

This PDF file includes:

Main Text
Figures 1 to 6

Supplementary material:
Figures S1 to S10
Tables S1 to S3
SI References

Abstract

Metabolism and biological functions of the nitrogen-rich compound guanidine have long been neglected. The discovery of four classes of guanidine-sensing riboswitches and two pathways for guanidine degradation in bacteria hint at hitherto overlooked but widespread sources of unconjugated guanidine in nature. So far, only three enzymes from a narrow range of bacteria and fungi have been shown to produce guanidine, with the ethylene-forming enzyme as the most prominent example. Here, we show that a related class of Fe^{2+}- and 2-oxoglutarate-dependent dioxygenases (2-ODD-C23) highly conserved among plants and algae catalyze the hydroxylation of homoarginine at the C6-position. Spontaneous decay of 6-hydroxyhomoarginine yields guanidine and 2-aminoadipate-6-semialdehyde. The latter can be reduced to pipecolate by pyrroline-5-carboxylate reductase but is more likely to be oxidized to aminoadipate by aldehyde dehydrogenase ALDH7B *in vivo*. Arabidopsis has three 2-ODD-C23 isoforms, among which Din11 is unusual because it also accepted arginine as substrate, which was not the case for the other 2-ODD-C23 isoforms from Arabidopsis or other plants. Guanidine contents were typically between 10 and 20 nmol*(g fresh weight)$^{-1}$ in Arabidopsis but increased to 100 or 300 nmol*(g fresh weight)$^{-1}$ after homoarginine feeding or treatment with Din11-inducing methyljasmonate, respectively. In 2-ODD-C23 triple mutants, the guanidine content was strongly reduced, whereas it increased in overexpression plants. We discuss the implications of the finding of widespread guanidine-producing enzymes in photosynthetic eukaryotes as a so far underestimated branch of the bio-geochemical nitrogen cycle and propose possible functions of natural guanidine production.

Introduction

Nitrogen availability is a limiting factor for productivity in many ecosystems and plants are the major contributors to assimilation of nitrogen into organic matter from inorganic precursors. The largest proportion of nitrogen is used in primary metabolism for the synthesis of proteins and nucleic acids. Additionally, many secondary metabolites that serve for internal signaling, adaptation or interactions with other organisms are nitrogen-containing molecules. Guanidine, which exclusively occurs as the protonated guanidinium cation under physiological conditions, has been discovered as a degradation product of guanine and arginine under chemically harsh conditions (Bénech & Kutscher, 1901; Strecker, 1861). Thirty-two years after its discovery in 1861, guanidine was detected in plants (Schulze, 1893). However, guanidine has no known function in plants, and it is unclear to which extent and how plants can synthesize and metabolize this nitrogen-rich compound (Marsden et al., 2015). In contrast, two enzymatic pathways for guanidine catabolism were recently discovered in bacteria and many bacteria express guanidine importers or exporters in response to externally supplied or internally produced guanidine (Funck et al., 2022; Nelson et al., 2017; Schneider et al., 2020; Sinn et al., 2021; Wang et al., 2021). Bacterial genes involved in guanidine metabolism are often regulated by members of four independent guanidine riboswitch classes, which may indicate an ancient evolutionary origin of guanidine metabolism (Lenkeit et al., 2020; Nelson et al., 2017; Salvail et al., 2020; Sherlock & Breaker, 2017; Sherlock et al., 2017).

Only two enzymes are known to release guanidine from arginine in side reactions. The arginine-4,5-desaturase NapI induces the decay of 5-hydroxyarginine to glutamate-5-semialdehyde (GSA) and guanidine when the initial hydroxylation occurs at the C5 atom of arginine instead of the C4 atom, where it would induce the desired desaturation of the C4-C5 bond (Dunham et al., 2018). The Ethylene Forming Enzyme (EFE) from *Pseudomonas savastanoi* converts 2-oxoglutarate (2-OG) into ethylene and this activity depends on structural changes induced by binding of arginine to the active site (Fukuda et al., 1992; Martinez et al., 2017). In a second reaction with roughly 50% turnover rate, EFE also catalyzes the hydroxylation of arginine at the C5 atom. Both enzymes belong to the class of Fe^{2+} and 2-OG-dependent dioxygenases (2-ODD), which use molecular oxygen to catalyze a broad range of reactions involving an Fe^{IV}-oxo-intermediate formed after the initial conversion of 2-OG to succinate (Farrow & Facchini, 2014; Hausinger, 2015; Herr & Hausinger, 2018). A third guanidine-producing enzyme, the guanylurea hydrolase GuuH from *Pseudomonas mendocina* strain GU, is from a different protein family and may have evolved recently to utilize guanylurea generated by metformin degradation (Tassoulas et al., 2021).

In plants, the family of 2-ODDs has diversified immensely, and it has been divided into three subfamilies according to sequence similarity and the types of reactions that the respective enzymes catalyze (Kawai et al., 2014; Prescott & John, 1996). Subfamily A comprises RNA demethylases and related enzymes, subfamily B comprises prolyl-hydroxylases that function in posttranslational protein modification, and the largest subfamily C comprises enzymes that act in the synthesis or modification of plant hormones, pigments and other secondary metabolites. Besides the 2-ODDs with known enzymatic function, subfamily C also contains many proteins of unknown function. Among these, Arabidopsis Din11 (Dark-induced11; At3g49620) has been identified because its expression was induced by prolonged dark treatment, which leads to C-starvation and the induction of autophagy (Fujiki et al., 2001; Magen et al., 2022). Din11 orthologs are encoded in the genomes of most analyzed plants and green algae, and Arabidopsis as well as many other *Brassicacea* express three paralogs of this protein: Din11, At3g49630 and At3g50210, among which At3g50210 seems to be the most ancestral form (Supplementary Fig. S1). In rice, the single Din11 ortholog has been named 2-ODD33 and was reported to have weak melatonin-2-hydroxylase activity (Byeon & Back, 2015). Because the numbering of the 2-ODDs in rice does not reflect their phylogenetic relationship and the phylogenetic study by Kawai et al (2014) used DOX as rather uncommon acronym for the 2-ODDs, we propose a hybrid nomenclature with 2-ODD followed by a denominator for the phylogenetic clade as defined in Kawai et al (2014). According to this

nomenclature, we propose 2-ODD-C23.1 as systematic name for At3g50210, 2-ODD-C23.2 for Din11 and 2-ODD-C23.3 for At3g49630.

An important N-containing class of secondary plant metabolites are non-proteinogenic amino acids, which may have metabolic, storage, defense, or signaling functions (Bell, 2003). Homoarginine, the C6-analog of arginine, is accumulated to high concentrations in seeds of several *Lathyrus* species, where it is assumed to be a nitrogen storage form that is not easily accessed by bacteria or insects (Bell, 1962; Bell, 1980; Lambein et al., 1992; Rao et al., 1963). Trace amounts of homoarginine were also detected in other plants, and in humans it is thought to interfere with nitric oxide production and signaling (Koch et al., 2022; Lambein et al., 2019; Sulser & Sager, 1976). In man and animals, homoarginine is produced from lysine and arginine in a side reaction of glycine amidinotransferase (Choe et al., 2013). A protein with similar activity has been isolated from *Lathyrus sativus*, but the molecular identity of this protein remains unknown and we did not detect a homolog of human glycine amidinotransferase in any annotated plant genome (Srivenugopal & Adiga, 1980). No other homoarginine-metabolizing enzymes have so far been reported from plants.

Here we describe the identification of plant 2-ODD-C23 isoforms as homoarginine-6-hydroxylases, which initiate the decay of 6-hydroxyhomoarginine to 2-aminoadipate-6-semialdehyde (AASA) and guanidine. Within the 2-ODD-C23 clade, we found Din11/2-ODD23.2 to be special because it accepted also arginine as substrate to produce 5-hydroxy-arginine. This finding identifies 2-ODD-C23s as the first eukaryotic enzymes that release free guanidine from conjugated precursors, an activity previously only known as side reaction of rare bacterial enzymes. AASA accumulation is toxic because it inactivates the enzyme cofactor pyridoxal-5-phosphate (PLP) by adduct formation, therefore, AASA is detoxified by oxidation to aminoadipate by ALDH7B4 (AASA-DH, At1g54100; (Končitíková et al., 2015; van Karnebeek et al., 2016)). In solution, AASA is in equilibrium with the cyclic δ^1-piperideine-6-carboxylate (P6C), which can be reduced to pipecolate by pyrroline-5-carboxylate reductase (P5CR) (Fujii et al., 2002; Struys et al., 2014). Our comparison of the activities of P5CR and ALDH7B4 indicates that under physiological conditions, the oxidation of AASA is the prevalent metabolic route in plants.

Results

Expression of plant EFE-like proteins causes guanidine production in *E. coli*

To determine if plant 2-ODD-C23 enzymes, which share the highest degree of similarity with EFE among the plant ODDs, also catalyze the production of guanidine, selected proteins were overexpressed in *E. coli*. We focused on the three 2-ODD-C23 isoforms from Arabidopsis (Din11/2-ODD-C23.2, At3g49630/2-ODD-C23.3 and At3g50210/2-ODD-C23.1) and the orthologs from rice and soybean, which are encoded by single-copy genes. We also included Ava5009 from *Anabaena variabilis* as representative of the most similar group of cyanobacterial 2-ODDs, although it is probably not orthologous to 2-ODD-C23 from plants and green algae. When we compared the annotation of Din11 with RNAseq data, we noticed that only very few RNAseq reads cover the 5′-end of the mRNA, whereas the coverage increases strongly 89 bp downstream of the predicted transcription start site, at a position 13 bp after the annotated start codon (Supplementary Fig. S2). A second ATG codon in the same reading frame is located 62 bp downstream of the major transcription start site. Comparison of the predicted protein sequences showed that the first 24 amino acids of the annotated Din11 (At3g49620.1, here termed Din11L) do not align with 2-ODD-C23 homologs from other plant species, whereas the variant starting with the second ATG codon (termed Din11s) aligns well over its entire length. Nevertheless, we were able to amplify the coding sequence of Din11L from Arabidopsis cDNA.

Of the three Arabidopsis 2-ODD-C23 isoforms, only the short variant of Din11 induced guanidine production when overexpressed in *E. coli* (Fig. 1). Guanidine production was stimulated by addition of arginine to the culture medium, whereas addition of 2-OG had no effect (Supplementary Fig.

S3). We speculated that the other 2-ODD-C23 isoforms might use a compound similar to arginine as substrate and supplemented the cultures with various other guanidine compounds known to occur in nature (methylguanidine, guanidinoacetate, guanidinopropionate, guanidinobutyrate, agmatine, homoarginine, taurocyamine). Only when the culture medium of the cells was supplemented with homoarginine, all 2-ODD-C23 isoforms from Arabidopsis except Din11L induced guanidine production in the *E. coli* cultures (Fig. 1). The 2-ODD-C23 orthologs from soybean and rice (2-ODD33) mediated homoarginine-dependent guanidine accumulation to a similar degree than Din11s and At3g50210. The guanidine concentration was very similar in the *E. coli* cells and in the supernatant, indicating that guanidine was exported from the cells until an equilibrium with the medium was reached (Supplementary Fig. S3). In contrast to the 2-ODD-C23 isoforms, the 2-ODD Ava5009 from the cyanobacterium *Anabaena variabilis* did not mediate guanidine production from arginine or homoarginine.

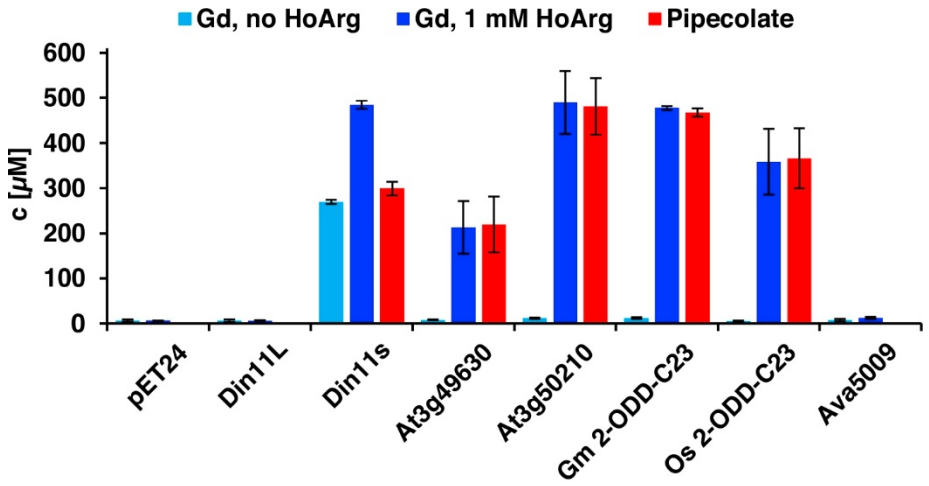

Fig. 1: Expression of 2-ODD-C23 isoforms induces guanidine accumulation in *E. coli*. The cDNAs of various 2-ODD-C23 from plants isoforms and Ava5009 from *Anabaena variabilis* were cloned in pET24 for overexpression of the respective proteins in *E. coli*. Protein expression was induced over night at 18 °C in LB medium supplemented with 0.2% (w/v) glucose and 10 μM Fe^{2+}. One aliquot of each culture was additionally supplemented with 1 mM homoarginine (HoArg). All cultures reached an OD around 10. For guanidine and pipecolate quantification by LC-MS, aliquots of the cultures were diluted in a 20-fold excess of methanol with 10 μM $^{13}C^{15}N$-labelled guanidine as analytical standard. Pipecolate was exclusively detected in the cultures supplemented with homoarginine. Columns are the average ±SD of samples from three independent cultures.

The detection of free guanidine indicated that 2-ODD-C23 might be homoarginine-6-hydroxylases, as 6-hydroxyhomoarginine is expected to decay spontaneously to yield guanidine and 2-aminoadipate-6-semialdehyde (AASA). The latter is in spontaneous equilibrium with δ^1-piperideine-6-carboxylate (P6C), which can be converted to pipecolate by P5CR (proC in *E. coli*, (Fujii et al., 2002)). Indeed, we detected pipecolate in the *E. coli* cultures in quantities proportional to the amount of guanidine (Fig. 1). Only in the cells expressing Din11s, the proportion of pipecolate was lower, indicating that Din11s used both arginine and homoarginine as substrates. In contrast to guanidine, pipecolate was predominantly retained inside the cells (Supplementary Fig. S3). By GC-MS analysis of the headspace of bacterial cultures expressing Din11s or At3g50210 and incubated with 5 mM arginine or homoarginine for 6 h in air-tight tubes, no ethylene production was detected (Supplementary Fig. S3). The guanidine concentration in the cultures was above 100 μM, indicating that there was enough oxygen in the tubes to allow enzyme activity.

Plant 2-ODD-C23 enzymes are homoarginine-6-hydroxylases

To determine if the Arabidopsis 2-ODD-C23 isoforms directly catalyze the release of guanidine from homoarginine, we purified the recombinant proteins by Ni-affinity chromatography. Measurement of the rate of O_2 consumption at variable substrate concentrations allowed the characterization of the three Arabidopsis enzymes (Fig. 2). With a fixed and saturating concentration of 0.5 mM 2-OG, At3g50210 had the lowest K_M for homoarginine (0.68 mM) and the highest specific activity (A_{max} = 17 nmol s^{-1} mg^{-1}). Din11s had a K_M of 1.68 mM for homoarginine and a lower specific activity (A_{max} = 10 nmol s^{-1} mg^{-1}). With a K_M of 4.8 mM and an A_{max} of 6 nmol s^{-1} mg^{-1}, At3g49630 had the lowest activity of the three Arabidopsis 2-ODD-C23 paralogs. LC-MS/MS analysis of the reaction products confirmed the formation of P6C, succinate and guanidine. When *O*-(2,3,4,5,6-Pentafluorbenzyl)-hydroxylamine was added during the reaction, the derivatization product of AASA was also detected. No products with the masses of dehydro-homoarginine or hydroxy-homoarginine were accumulating in the reaction mixture. We concluded that all three Arabidopsis 2-ODD-C23 isoforms specifically catalyze the C6-hydroxylation of homoarginine, which is followed by the spontaneous decay to guanidine and AASA, which subsequently cyclizes to P6C. As expected from the analysis of the *E. coli* cultures, only Din11s showed O_2 consumption also with arginine, although the K_M (3.3 mM) was higher compared to homoarginine and the specific activity was lower (A_{max} = 3 nmol s^{-1} mg^{-1}). Neither lysine nor

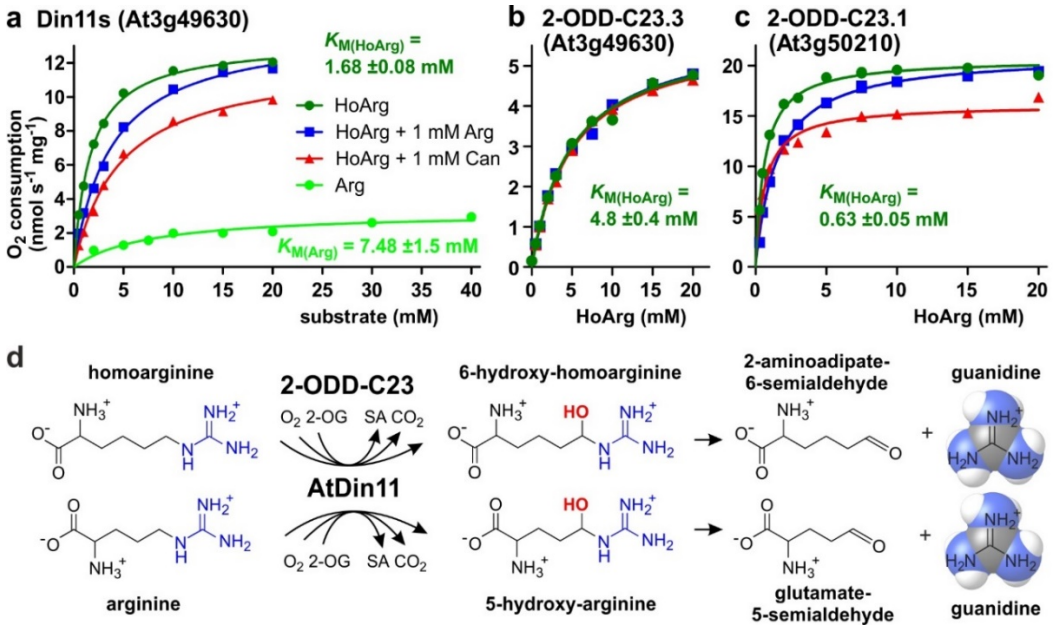

Fig. 2: Kinetic analysis of purified recombinant 2-ODD-C23 isoforms. (a)-(c) Specific activities of oxygen consumption at various substrate and inhibitor concentrations were analyzed with a Clark-type electrode. The concentration of the co-substrate 2-oxoglutarate was fixed at 0.5 mM. Only Din11s showed oxygen consumption with both homoarginine (HoArg) or arginine (Arg). The reaction of Din11s and At3g50210 with homoarginine was inhibited in the presence of 1 mM arginine (blue lines) or canavanine (red lines). Specific activities were calculated from the slope of the initial linear reaction rate. K_M, and A_{max} were determined by non-linear regression (see also Supplementary Table S1). Data points represent single measurements, consistent results were obtained with independent enzyme preparations. (d) Reactions catalyzed by 2-ODD-C23 isoforms with subsequent spontaneous decay of the reaction products.

agmatine or any other guanidine-containing compound induced O_2 consumption with one of the purified enzymes. The reaction of Din11s with arginine yielded guanidine and GSA with its cyclic

counterpart δ^1-pyrroline-5-carboxylate (P5C), indicating that arginine is hydroxylated at the C5 position as in EFE from *Pseudomonas savastanoi* (Fukuda et al., 1992).

When we tested the effect of 1 mM arginine on the reaction of the 2-ODD-C23 isoforms with homoarginine, we detected a competitive inhibition of Din11s and At3g50210, whereas At3g49630 was insensitive to arginine (Fig. 2 and Supplementary Fig. S4). We further tested the effect of the arginine antimetabolite canavanine on the reaction of the 2-ODD-C23 isoforms. Canavanine is the 5-oxa-analog of arginine and therefore cannot be hydroxylated at this position. Similar to arginine, which is both substrate and inhibitor for Din11s, canavanine showed competitive inhibition of the reaction of Din11s with homoarginine. In contrast, the inhibition of At3g50210 was of the mixed type and At3g49630 was not inhibited by canavanine.

When the concentration of the co-substrate 2-oxoglutarate was varied at near-saturating concentration of homoarginine (10 mM), all three 2-ODD-C23 isoforms showed K_M values between 20 and 100 µM and the reaction was inhibited by high 2-OG concentrations (Supplementary Fig. S4 and Supplementary Table S1). For At3g50210 we determined the pH-dependence of the enzymatic reaction and observed maximal activity around pH 7.2 (Supplementary Fig. S4), whereas the enzyme was virtually inactive below pH 5 and above pH 9.

Arabidopsis 2-ODD-C23 isoforms are cytosolic enzymes and mediate guanidine production *in vivo*

The protein sequences of the 2-ODD-C23 isoforms from Arabidopsis do not contain any recognizable targeting signals. Consistently, the analysis of plants expressing 2-ODD-C23:GFP fusion proteins under control of the constitutive UBQ10-promoter demonstrated the cytosolic localization of all three isoforms (Fig. 3). Among 41 plants transformed with a construct for expression of Din11L:GFP, no plants with detectable GFP fluorescence were identified. Among 80 lines carrying a construct for expression of Din11s:GFP, several lines showed cytosolic GFP signals but only in one line, the expression of Din11s:GFP was stable over several generations. For both At3g49630:GFP and At3g50210:GFP, several independent lines were identified that stably expressed the GFP fusion protein. GFP signals were typically strongest in At3g50210:GFP-expressing plants.

In order to determine whether the 2-ODD-C23 isoforms catalyze C6-hydroxylation of homoarginine under physiological conditions, we identified and generated Arabidopsis mutants. Several T-DNA insertion lines were obtained from the Nottingham Arabidopsis Stock Centre and were backcrossed at least 3 times to Col-0 wildtype (WT) plants to obtain single insertion lines (Supplementary Fig. S5 and Supplementary Table S2). Because *Din11* and *At3g49630* are located directly next to each other on chromosome 3, we used mutagenesis with CRISPR/Cas9 with a gRNA targeting the third exon of both *Din11* and *At3g49630* to generate double mutants. We obtained one line, in which the 5′-end of *Din11* is fused to the 3′-part of *At3g49630*. Insertion of 1 bp at the fusion site causes a frame shift and inactivates both genes. A second line contains a 27 bp deletion including the border between intron 2 and exon 3 of *Din11* and a 1 bp deletion in exon 3 of *At3g49630*. The CRISPR/Cas9-generated mutants also were backcrossed to WT plants to eliminate the CRISPR/Cas9 expression cassette and potential off-target mutations. To generate triple mutants, the double mutants were crossed with the mutant line *at3g50210-1*, which carries a T-DNA insertion in the third exon of At3g50210. All single, double, and triple mutants were phenotypically not different from WT plants when growing under normal conditions in sterile culture or in the greenhouse.

Basal guanidine contents were around 10-15 nmol [g fresh weight (Fw)]$^{-1}$ equivalent to 100-200 nmol (g dry weight)$^{-1}$ in the rosettes of axenically grown Arabidopsis WT plants and were increased to 20-30 nmol (g Fw)$^{-1}$ in 2-ODD-C23:GFP overexpressing plants (Fig. 4). The guanidine content of soil grown plants was usually slightly higher, and in legume seeds and

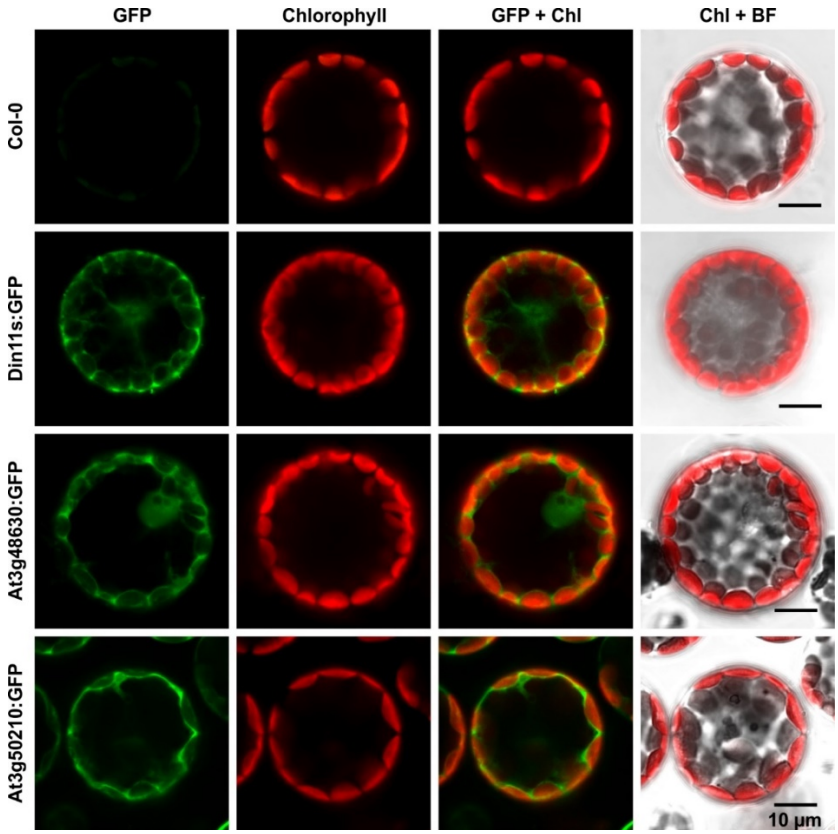

Fig. 3: Subcellular localization of 2-ODD-C23 isoforms. Protoplasts were isolated from plants expressing 2-ODD-C23:GFP fusions under control of the constitutive UBQ10-promoter. Spectrally resolved confocal fluorescence images were used to separate GFP (depicted in green) fluorescence from chlorophyll autofluorescence (Chl, depicted in red). BF, brightfield image.

seedlings we detected up to 2.4 µmol (g dry weight)$^{-1}$ (equivalent to 145 ppm) guanidine (Supplementary Fig. S6). The guanidine content in rosettes of 2-ODD-C23-triple mutants was consistently lower than in WT plants. Surprisingly, the basal homoarginine content (10-20 nmol (g Fw)$^{-1}$ in WT rosettes) was reduced to around 5 nmol (g Fw)$^{-1}$ in rosettes of both the triple mutants as well as in At3g50210:GFP overexpressing plants (Fig. 4). When WT plants and At3g50210:GFP-expressing plants were transferred to culture plates with 0.2 mM homoarginine in the medium, they accumulated both homoarginine and guanidine in a time-dependent manner, reaching 100 nmol (g Fw)$^{-1}$ guanidine in WT rosettes and 600 nmol (g Fw)$^{-1}$ in the rosettes of the overexpressor plants. Like WT and overexpressor plants, the 2-ODD-C23 triple mutants accumulated homoarginine to around 800 nmol (g Fw)$^{-1}$, whereas the guanidine content in the rosettes stayed nearly unchanged. In *din11* and *at3g49630* single mutants, the guanidine content was not reduced compared to WT plants after external supply of homoarginine. In *at3g50210* single mutants, however, the guanidine content was as low as in the triple mutants (Supplementary Fig. S5).

Addition of homoarginine or arginine to the growth medium impaired root growth of Arabidopsis seedlings (Supplementary Fig. S7). On media containing either 1 mM arginine or 0.1 mM homoarginine, the roots of 1-week old plants had only half the length of the roots of control plants grown without amino acid supplement. Above 0.2 mM homoarginine, also the growth of the rosettes was impaired (Supplementary Fig. S7). However, these inhibitory effects were not changed in the 2-ODD-C23 triple mutants and 2-ODD-C23:GFP overexpressing plants, indicating that hydroxylation of homoarginine likely does not serve to detoxify high concentrations of

homoarginine. Addition of 1 mM guanidine to the growth medium had no effect on seedling growth, whereas 5 mM guanidine was lethal (Supplementary Fig. S7 and data not shown).

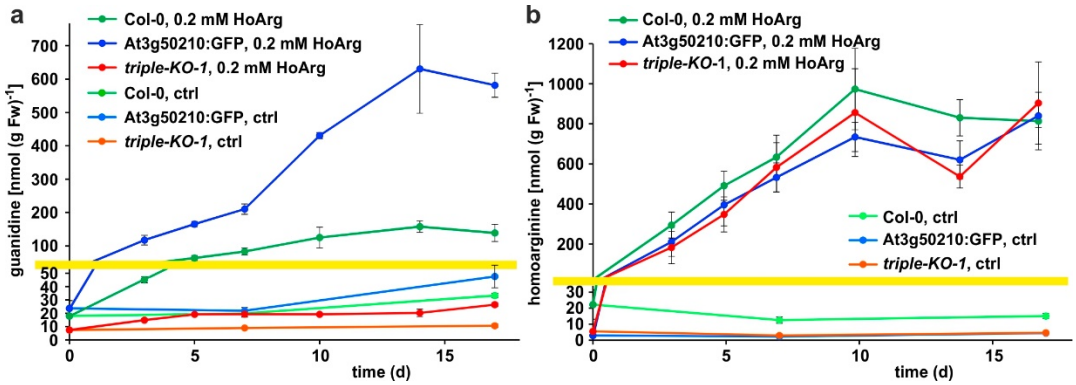

Fig. 4: Guanidine and homoarginine contents in leaves of Arabidopsis plants. Plants were grown for two weeks in sterile culture and transferred to fresh plates with 0.2 mM or without (ctrl) homoarginine. Guanidine (a) and homoarginine (b) were extracted from rosettes in 80% (v/v) methanol containing $^{13}C^{15}N$-labelled guanidine as analytical standard and quantified by LC-MS. Col-0, wildtype; At3g50210:GFP, At3g50210:GFP overexpressing plants, triple-KO, 2-ODD-C23 triple mutant. The yellow line marks a change in the scale of the Y-axis. Error bars indicate SD from four plant samples. The entire experiment was repeated with consistent results.

Originally, Din11 was named for its induction by prolonged darkness, a condition now understood to induce both C-starvation and autophagy. However, we did not detect phenotypical differences between *din11* or triple mutants and WT plants after prolonged dark treatment (Fig. 5). It had further been reported that expression of Din11 was induced by treatment with methyljasmonate (MeJA) (Caarls et al., 2017) and by perturbations of ROS homeostasis (Gadjev et al., 2006),

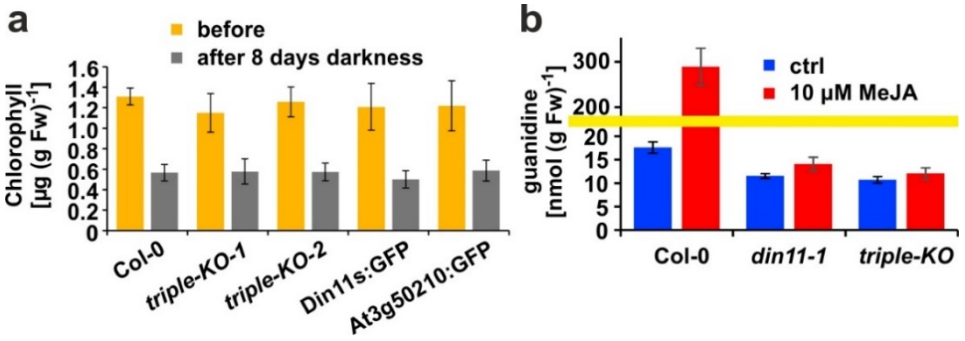

Fig. 5: Effect of darkness and methyljasmonate (MeJA) on 2-ODD-C23 mutants. (a), Eight-day-old seedlings grown under short-day conditions were placed for 8 days in permanent darkness. Chlorophyll was extracted before and after the dark treatment and quantified spectrometrically. Col-0, wildtype; triple-KO, 2-ODD-C23 triple mutant; Din11s:GFP, At3g50210:GFP, plants overexpressing 2-ODD-C23:GFP fusion proteins. Error bars indicate SD of N = 8 independent plant samples. (b), Three-week-old plants were treated for one week with approximately 50 µM MeJA by applying a stock solution in 50% (v/v) ethanol to the lid of the Petri dishes. Guanidine was extracted from rosettes in 80% (v/v) methanol containing $^{13}C^{15}N$-labelled guanidine as analytical standard and quantified by LC-MS. *din11-1*, single T-DNA insertion mutant of *Din11*. The yellow line marks a change in the scale of the Y-axis. Error bars indicate SD of 4 independent plant samples. The *din11-2* mutant line and the independently generated second triple mutant gave consistent results.

whereas analysis of publicly available RNAseq data did not reveal a treatment that induced all three Arabidopsis 2-ODD-C23 isoforms (Supplementary Fig. S8) (Zhang et al., 2020). Treatment of WT

plants with 10 or 50 µM MeJA did not induce consistent and marked changes of the content of homoarginine and arginine in the rosettes of Arabidopsis seedlings. However, MeJA treatment strongly induced the guanidine content in Arabidopsis rosettes and this induction was lost in *din11* single mutants and not decreased much further in 2-ODD-C23 triple mutants (Fig. 5).

Metabolic fate of AASA in plants

The different rates of homoarginine metabolism in WT plants, triple mutants and At3g50210:GFP overexpressing plants, as evidenced by different levels of guanidine accumulation, were surprisingly not reflected in different rates of homoarginine accumulation after external supply (Fig. 4). Therefore, we wondered if AASA/P6C production by 2-ODD-C23 might serve a signaling rather than a metabolic function. As in the *E. coli* cultures, P5Cr might convert AASA/P6C to pipecolate, which is the direct precursor for the mobile defense signal N-hydroxypipecolate (Zeier, 2021). Purified, recombinant plant P5CR converted P6C to pipecolate with a K_M of 173 ±18 µM or 257 ±23 µM and an A_{max} of 7 or 13 nmol s^{-1} mg^{-1}, when NADH or NADPH were used as electron donors, respectively (Fig. 6). An alternative route for AASA/P6C metabolism would be oxidation of AASA to aminoadipate by an aldehyde dehydrogenase. For maize and pea, it was shown that ALDH7B4 has a high affinity for AASA (Končitíková et al., 2015). Indeed,

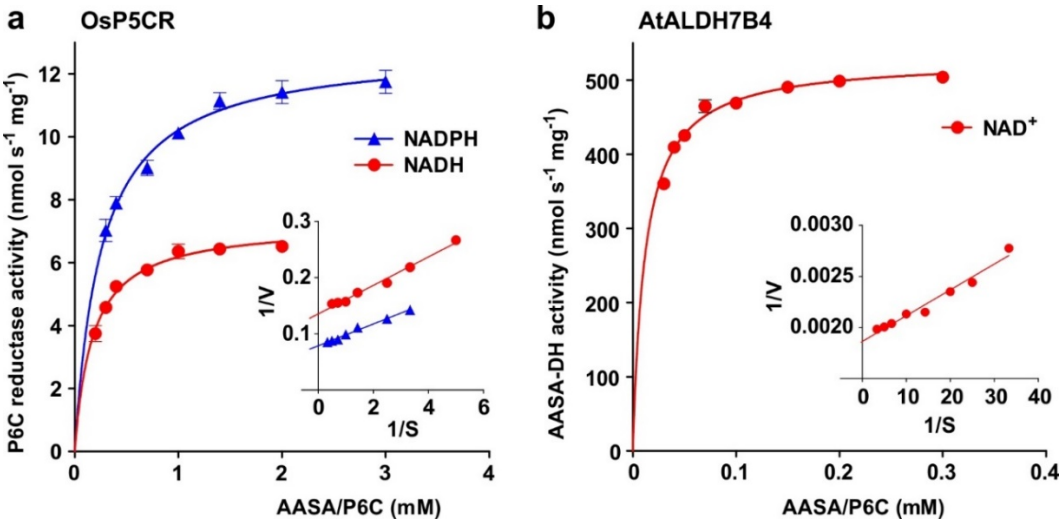

Fig. 6: Reduction and oxidation of AASA/P6C by plant enzymes. Recombinant purified enzymes were used to compare the reduction of P6C to pipecolate by pyrroline-5-carboxylate reductase from rice (OsP5CR; a) with the oxidation of AASA by Arabidopsis aldehyde dehydrogenase 7B4 (ALDH7B4; b) at 35 °C with a fixed cofactor concentration of 1 mM. OsP5CR used either NADH or NADPH as electron donor for the conversion of P6C to pipecolate. ALDH7B4 had a much higher specific activity and a lower K_M, but efficiently catalyzed the reaction of AASA to aminoadipate only with NAD^+ as electron acceptor. Data points are the average ±SD of technical triplicates. Colored lines represent the fit of the experimental data to the Michaelis-Menten equation. The insets show the Lineweaver-Burk plots of the same data. All experiments were repeated with an independent enzyme preparation and showed consistent results.

purified, recombinant AtALDH7B4 (At1g54100) converted AASA to aminoadipate with a K_M of 11.9 ±1.0 µM and an A_{max} of 529 ±6 nmol s^{-1} mg^{-1} with NAD^+ as electron acceptor. For the cofactor NAD^+, ALDH7B4 had a K_M of 324 ±17 µM, whereas the enzyme was almost inactive with $NADP^+$ as electron acceptor and neither was NADPH formation linear over time nor did it show a linear correlation with the amount of enzyme (Supplementary Fig. S9). ALDH7B4 also accepted GSA/P5C as substrate, but the conversion rates were 60 times lower compared to AASA/P6C and also in this case, the reaction rate was not linearly correlated to the amount of enzyme (Supplementary Fig. S9). The 10-fold lower K_M of AASA oxidation to aminoadipate *vs.* P6C

reduction to pipecolate suggests that the oxidative route is predominantly occurring under physiological conditions. Independent of genotype and homoarginine supply, the pipecolate content of seedlings was below 2 nmol (g Fw)$^{-1}$ under our conditions and could not be quantified because the peak was not clearly separated from other compounds with the same M/Z ratios. The aminoadipate content in Arabidopsis rosettes was also below the level for reliable quantification [1 nmol (g Fw)$^{-1}$] but increased to almost 6 nmol (g Fw)$^{-1}$ in At3g50210:GFP-overexpression plants after supply of external homoarginine (Supplementary Fig. S10). This increase was absent in 2-ODD-C23 triple mutants and barely detectable in WT plants, indicating that aminoadipate metabolism is faster than the production via AASA derived from homoarginine hydroxylation by 2-ODD-C23.

Discussion

In this study, we discovered a novel enzymatic activity for a previously uncharacterized clade of plant 2-ODDs. All analyzed 2-ODD-C23 proteins mediated the hydroxylation of homoarginine at the C6 position, thereby inducing its decay to AASA and guanidine (Fig. 2). This is in sharp contrast to *P. savastanoi* EFE, which was virtually inactive with homoarginine (Martinez & Hausinger, 2016). The K_M values for homoarginine hydroxylation by the plant enzymes were higher than the K_M of *P. savastanoi* EFE for arginine (50 µM) and the A_{max} values were intermediate between the values for ethylene formation (54 nmol s^{-1} mg^{-1}) and arginine hydroxylation (1.2 nmol s^{-1} mg^{-1}) reported for EFE (Martinez & Hausinger, 2016). Among the biochemically characterized plant 2-ODDs from class C, DMR6/S5H had a lower K_M (5.1 ±1.4 µM) and a similar A_{max} (5.9 ±1.1 nmol s^{-1} mg^{-1}) for salicylate hydroxylation (Zhang et al., 2017). Din11, which is exclusively present in *brassicaceae*, additionally accepted arginine as substrate. Although Din11 has a lower specific activity and a higher K_M for the reaction with arginine, the low concentration of homoarginine in Arabidopsis may lead to a preferential hydroxylation of arginine by Din11. 2-ODD33, the 2-ODD-C23 ortholog from rice, was previously reported to have melatonin-2-hydroxylase activity (Byeon & Back, 2015). However, the reported rate of 2-hydroxymelatonin accumulation by purified, recombinant 2-ODD33 was 1000-fold lower than the hydroxylation of homoarginine in our experiments, indicating that homoarginine is the preferred substrate of 2-ODD-C23 enzymes.

The evolutionary origin of 2-ODD-C23 function is at present ambiguous. Loss of the gene in *Chlamydononas reinhardtii* has previously led to the interpretation that these enzymes were specific to plants (Kawai et al., 2014). However, putative orthologs of 2-ODD-C23 are present in other green algae, whereas the protein with the highest degree of similarity in the cyanobacterium *Anabaena variabilis* (Ava5009) did not have homoarginine-6-hydroxylase activity when expressed in *E. coli* (Fig. 1). It is thus conceivable that the production of guanidine from homoarginine or arginine evolved in photosynthetic eukaryotes. The single-copy 2-ODD-C23 isoforms from rice and soybean accepted exclusively homoarginine as substrate, indicating that arginine hydroxylation by Arabidopsis Din11 derived from neofunctionalization after at least two duplication events in the *Brassicaceae* family (Supplementary Fig. S1). Sequence alignments between bacterial and fungal EFEs and plant 2-ODDs did not reveal a close relationship between Din11 and EFE (data not shown), indicating an independent evolution of arginine-5-hydroxylase activity in both enzymes.

The guanidine content was strongly reduced mutant plants devoid of 2-ODD-C23 expression, indicating that 2-ODD-C23s are the major source of free guanidine in Arabidopsis. At3g50210 mediated the major part of the homoarginine-dependent guanidine production (Supplementary Fig. S5) which is consistent with the highest specific activity (Fig. 2) and the highest basal expression level of At3g50210 (Supplementary Fig. S8). In contrast, Din11 expression has the highest dynamic range and induction of Din11 by MeJA induced a strong increase in guanidine production, presumably from arginine as precursor (Fig. 5). This increase was virtually absent in *din11* single mutants and the triple mutants, indicating that it was exclusively attributable to Din11 activity. Based

on a basal guanidine content of 120 nmol (g dry weight)$^{-1}$ (equivalent to 7 ppm) in Arabidopsis and our observation that other plants have similar or even higher contents of guanidine (Supplementary Fig. S6), we estimated the global annual production of guanidine by plants. With a total annual biomass production of $5*10^{10}$ t by land plants, this estimation yields an annual guanidine production of $3.5*10^{5}$ t by plants, corresponding roughly to the 2.5-fold of the industrial production in 2016 (Precision Reports, 2021).

Plants were shown to transport but barely metabolize guanidine (Marsden et al., 2015), indicating that nitrogen released as guanidine cannot be efficiently recycled by plants. Considering the often growth-limiting function of nitrogen for plants, this raises the question whether guanidine may serve as a defense or signaling compound. In soil, a greater proportion of bacteria contains genes for guanidine import and assimilation than among bacteria associated with human skin or the gut, which preferentially contain genes for guanidine exporters (Sinn et al., 2021). Since bacteria differ in their responses to guanidine, it is possible that guanidine accumulation or even secretion is a way for plants to modulate their microbiomes (Sharma et al., 2023). A similar function was proposed for hydroxyguanidine that was secreted by *Pseudomonas canavaninivorans* after degradation of plant-produced canavanine (Hauth et al., 2022). Induction of Din11 expression and guanidine production by wounding and MeJA may also point to a function of guanidine in the defense against or repulsion of herbivores (Caarls et al., 2017; Griffiths, 2020). Expression of Din11 was additionally induced in several mutants or after treatments that cause ROS accumulation, indicating that ROS may act as second messenger in the induction of Din11 expression (Supplementary Fig. S8) (Gadjev et al., 2006). Further studies will be required to determine the biological purpose of guanidine production from homoarginine or arginine by 2-ODD-C23 enzymes.

In addition or alternatively, the second reaction products of 2-ODD-C23s, AASA/P6C or GSA/P5C could represent physiologically functional products. GSA/P5C produced by cytosolic Din11 (Fig. 3) is most likely converted to proline by P5CR, which is a cytosolic enzyme in plants as well (Funck et al., 2012). Thereby, the activity of Din11 may explain the observation that besides glutamate also arginine can serve as precursor for proline synthesis in plants (Adams & Frank, 1980; Winter et al., 2015). So far, no combination of enzymes residing in the same compartment was known that could catalyze the conversion of arginine to proline without glutamate as intermediate (Trovato et al., 2019). However, the exclusive occurrence of Din11 orthologs in *brassicaceae* indicates that this metabolic pathway is not common among plants (Supplementary Fig. S1). The maximal guanidine concentration of 400 nmol (g Fw)$^{-1}$ observed in MeJA-treated Arabidopsis plants (Fig. 5) argues against a major contribution to stress-induced proline accumulation, which typically reaches 5-10 µmol (g Fw)$^{-1}$ (Forlani et al., 2019). Besides the induction by MeJA, expression of Din11 was also induced by prolonged dark treatment, which led to its initial identification and naming (Fujiki et al., 2001). Prolonged dark treatment causes C-starvation in plants and results in the induction of autophagy to mobilize energy by breakdown of cellular components and organelles (Magen et al., 2022). Degradation of homoarginine by 2-ODD-C23s is unlikely to be a relevant contribution to energy production during C-starvation because the observed homoarginine content was very low in Arabidopsis (Fig. 4). In contrast, degradation of arginine via Din11 to GSA/P5C and guanidine may serve to mobilize the C-skeleton of arginine without overloading the nitrogen metabolism. Degradation of arginine via arginase to ornithine and urea would result ultimately in glutamate and ammonia formation by glutamate dehydrogenase and urease (Winter et al., 2015). High ammonia concentrations are toxic for plants, especially when the energy or the enzymes to re-assimilate it into glutamine are lacking (Moreira et al., 2022). However, the extent of chlorophyll degradation was not different between WT plants, 2-ODD-C23 triple mutants and overexpressing plants, indicating that the efficiency of autophagy in remobilizing carbon and nitrogen does not depend on 2-ODD-C23 activity (Fig. 5). We are not aware of any reports describing a function of homoarginine in plants except the storage and defense function in seeds of hyperaccumulating *Lathyrus* species (Bell, 1980). The unexpected reduction of the homoarginine content in both, 2-ODD-C23 overexpression plants and 2-ODD-C23 triple mutants in Arabidopsis may indicate the existence of an auto-regulatory signaling loop.

AASA originating from the decay of 6-hydroxyhomoarginine can be converted to pipecolate by P5CR after spontaneous cyclisation to P6C (Fujii et al., 2002; Struys et al., 2014). In this way, 2-ODD-C23s might contribute to the production of the mobile defense signal N-hydroxypipecolate (Zeier, 2021). However, the direct comparison of the kinetic properties of P5CR and ALDH7B4 suggested that oxidation of AASA to aminoadipate by ALDH7B4, which is a shared reaction with the lysine degradation pathway, is the main pathway under physiological conditions (Fig. 6) (Arruda & Barreto, 2020). We did not find information about the rate of AASA-cyclisation to P6C or the equilibrium concentrations in plants. In human plasma from patients with ALDH7A1 defects, approximately equal concentrations of both compounds were detected after FMOC-derivatization (Xue et al., 2019). Consistent with the kinetic properties of P5CR and ALDH7B4, no increase of the pipecolate content after feeding with external homoarginine was observed in Arabidopsis plants overexpressing the 2-ODD-C23 isoform At3g50210 (Supplementary Fig. S10). Instead, a small increase in aminoadipate content was observed, indicating that AASA was indeed oxidized by ALDH7B4, but the rate of aminoadipate metabolism apparently exceeded the rate of synthesis by 2-ODD-C23 and ALDH7B4. *E. coli* lacks a specific AASA-DH and consequently cyclisation to P6C followed by reduction to pipecolate by the constitutively expressed P5CR (proC) is the main route of homoarginine metabolism by 2-ODD-C23 expressing *E. coli* cells (Fig. 1).

In humans, homoarginine is formed from lysine and arginine by mitochondrial glycine amidinotransferase (Choe et al., 2013). It is discussed that homoarginine interferes with NO production from arginine and thus might be an important regulator of NO signaling (Koch et al., 2022). Plants seem to lack NO synthases that use arginine as substrate and do not have proteins with significant sequence similarity to glycine amidinotransferase, although a protein with similar activity has been isolated from *Lathyrus sativus* seedlings (León & Costa-Broseta, 2020; Srivenugopal & Adiga, 1980). Thus, the biosynthesis and physiological function of homoarginine in plants will need to be addressed in future studies. In humans, the accumulation of AASA as consequence of mutations in ALDH7A1/Antiquitin, which is the ortholog of Arabidopsis ALDH7B4, leads to developmental retardation and epilepsy (Bouchereau & Schiff, 2020; Brocker et al., 2013). The disease symptoms are caused by formation of adducts of AASA with pyridoxal-5-phosphate, thereby inactivating pyridoxal-5-phosphate-dependent enzymes. In plants, ALDH7B enzymes may similarly serve to detoxify AASA derived from homoarginine hydroxylation by 2-ODD-C23s or from lysine degradation by the bifunctional lysine-ketoglutarate reductase/saccharopine dehydrogenase (LKR/SDH, At4g33150) (Arruda et al., 2000; Goncalves-Butruille et al., 1996). Mutation of Arabidopsis ALDH7B4 was reported to increase drought and salt sensitivity, whereas the sensitivity to herbicides was not significantly altered (Gil-Monreal et al., 2017; Kotchoni et al., 2006). In rice, mutation of ALDH7B6 reduced seed viability and caused the accumulation of pigments in the endosperm (Shen et al., 2012; Shin et al., 2009). Our analyses show that Arabidopsis ALDH7B4 has an even lower K_M (11.9 µM, Fig. 6) for AASA than the previously analyzed orthologs from rice and pea (97 and 89 µM respectively; (Končitíková et al., 2015)). It remains to be determined if ALDH7B4 functions specifically to prevent AASA accumulation or if it additionally acts nonspecifically on a broad range of aldehydes and semialdehydes.

Overall, our characterization of plant 2-ODD-C23s as homoarginine-6-hydroxylases is to our knowledge the first description of eukaryotic enzymes that mediate the production of guanidine. Although homoarginine represents a low abundant metabolite of unknown function and origin in most analyzed plants, the large amount of plant biomass produced every year implies that substantial amounts of guanidine enter the biological nitrogen cycle via the action of 2-ODD-C23 enzymes. The second product of 6-hydroxyhomoarginine decay, AASA/P6C, was primarily fed into the lysine degradation pathway by ALDH7B. So far, Din11 from Arabidopsis was the only 2-ODD-C23 isoform that accepted also the abundant arginine as substrate, but its low expression level and low specific activity apparently prevented excessive diversion of arginine towards guanidine and proline production. Consistently, the reduced guanidine and homoarginine contents were so far the only phenotypical difference that we detected in Arabidopsis mutants lacking all three 2-ODD-C23 isoforms. Although neither homoarginine nor guanidine are highly abundant metabolites in

Arabidopsis, the observed differences in the triple mutants and overexpressor plants confirm that the 2-ODD-C23 isoforms catalyze homoarginine hydroxylation *in vivo* and that potentially also production of homoarginine is a regulated process. Induction of Din11 by prolonged dark treatment, wounding, and reactive oxygen species provides hints that guanidine, AASA, or GSA may function in defense responses or other biotic interactions. We speculate that plants use guanidine production to influence guanidine-sensing or guanidine-assimilating microbes and plan to test this hypothesis in future studies.

Materials and Methods

DNA constructs and recombinant protein production

Bacterial expression constructs for Arabidopsis Din11, At3g49620, At3g50210, and ALDH7B4, as well as Os2-ODD33 and Gm2-ODD-C23 were generated by amplifying the coding sequence from cDNA with primers that introduce overlaps with a modified pET vector containing an N-terminal His-tag and a TEV cleavage site (Supplementary Table S3). The resulting PCR products were fused with the linearized vector by Gibson assembly (NEBuilderHiFi). Protein expression in *E. coli* SoluBL21 cells was induced with 1 mM IPTG at 18 °C overnight. The cells were lysed by sonication in extraction buffer (50 mM Hepes pH 7.5, 50 mM NaCl, 1x protease inhibitor cocktail (EDTA-free cOmplete, Roche) and the His-tagged proteins were purified with HisBind NiNTA-agarose (Qiagen) according to the recommendations of the supplier. Imidazole was removed from the purified proteins by passage through PD MidiTrap G-25 columns (GE lifescience) equilibrated with extraction buffer. Protein concentrations were determined according to Bradford (1976) with BSA as standard. All activity assays were performed with enzymes purified from at least three independent bacterial cultures.

Enzyme activity assays

Activity of ODDs was measured by following the oxygen consumption at 30 °C in a Clark-type electrode (Hansatech Oxygraph+) calibrated according to the instructions of the supplier. The reaction mix contained 50 mM MOPS pH 7.2, 70 mM NaCl, 20 mM KCl, 0.4 mM Na-ascorbate, 40 µM $Fe(NH_4)_2(SO_4)_2$, and variable concentrations of substrate or cosubstrate. The reactions were started by adding the purified enzymes and the specific activities were calculated from the difference between the oxygen consumption rate in the initial linear phase and the rate observed prior to the addition of the enzymes (typically around -20 nmol O_2 ml^{-1} s^{-1}, corresponding to 1 to 2% of the maximal rate in the presence of enzyme).

The activity of P5CR was calculated from the difference in the rates of NAD(P)H oxidation at pH 7.5 and 35 °C in the presence or absence of DL-P5C or L-P6C as described previously (Forlani et al., 2015). DL-P5C was synthesized by the periodate oxidation of δ-allo-hydroxylysine (Sigma H0377) and purified by cation-exchange chromatography, as described previously (Forlani et al., 1997). L-P6C generation from L-allysine ethyleneacetal (Sigma-Aldrich 714208) roughly followed a previous protocol (de La Fuente et al., 1997). A solution of 50 mg allysine ethyleneacetal in 5 ml water was mixed with 300 mg amberlite IR120 (Fluka 06428) and gently stirred for 20 min. The supernatant was discarded and the resin was loaded into a mini-column, washed with 10 mL of water and eluted with 10 mL of 1 M HCl in 1 ml fractions. The concentration of P6C was measured by mixing a proper dilution in 60 µl with 120 µl 1 mg ml^{-1} *o*-aminobenzaldehyde in ethanol, and the increase of absorbance at 465 nm was followed until a plateau was reached. The extinction coefficient of ε_{465} = 2800 M^{-1} cm^{-1} was used (Fothergill & Guest, 1977). Both DL-P5C and L-P6C were kept as stocks in 1 M HCl at 4 °C in the dark and neutralized with 1 M Tris-base immediately before use. The standard enzyme assay contained 50 mM Tris-HCl, 0.5 mg ml^{-1} NAD(P)H and 2 mM DL-P5C or 1 mM L-P6C. The activity of ALDH7B4 was calculated from the difference in $NAD(P)^+$ reduction at pH 7.5 and 35 °C in the presence or absence of variable concentrations of DL-P5C or L-P6C. The

standard reaction mixture contained 50 mM Tris-HCl, pH 7.5, 1 mM $NAD(P)^+$ and 2 mM DL-P5C or 1 mM L-P6C. The extinction coefficient of ε_{340} = 6.22 mM^{-1} cm^{-1} for NADH and NADPH was used to calculate specific activities.

Plant material, plant transformation and cultivation conditions

Arabidopsis [*Arabidopsis thaliana* (L.) Heynh.], ecotype Col-0 and T-DNA insertion lines (Supplementary Table S2) were obtained from the NASC. Surface-sterilized seeds were sown on solid half-strength Murashige and Skoog medium including Gamborg B5 vitamins (pH 5.8, supplemented with 2% [w/v] sucrose and 0.8% agar) in Petri dishes sealed with Leukopor tape (Leukoplast) and cultivated under a long-day light regime (16 h photoperiod; 110 µmol m^{-2} sec^{-1} at 21 °C). For seed production, seedlings were transferred to commercial substrate ("Einheitserde", type P, Gebr. Patzer, Sinntal-Altengronau, Germany) and cultivated in a greenhouse under long-day conditions. All T-DNA insertion mutants were backcrossed at least three times with WT plants, until the segregation pattern was consistent with a single T-DNA insertion. Constructs for the expression of GFP fusion proteins were obtained by inserting the coding sequences into pENTRa1 (Invitrogen) followed by LR-recombination with pUBC-GFP-Dest (Grefen et al., 2010). The construct for simultaneous CRISPR/Cas9-mediated inactivation of *Din11* and *At3g49630* was generated by ligating two matching oligonucleotides (Supplementary Table S3) into the BsaI-linearized vector pHEE401E (Wang et al., 2015). The resulting gRNA matches a Cas9 cleavage site in both genes with one mismatch in Din11 and no strongly predicted off-targets. All constructs were introduced into Arabidopsis plants by floral dip with *Agrobacterium tumefaciens* strain GV3101 (Clough & Bent, 1998). Transgenic plants were selected by spraying of seedlings with BASTA solution (50 µg ml^{-1}) or growth on sterile culture plates containing 30 µg ml^{-1} hygromycin B (Sigma). For the GFP constructs, lines with stable expression and a single-copy T-DNA insertion were selected by segregation analysis. CRISPR/Cas9-induced mutations were detected by high-resolution melting analysis using gene-specific primers (Supplementary Table S3) and confirmed by sequencing of the PCR products. The CRISPR/Cas9 construct was eliminated by backcrossing to WT plants. The absence of functional transcripts was confirmed by RT-PCR and sequencing of the products.

For feeding experiments, homoarginine or arginine were added to the culture medium from filter-sterilized stocks (100 mM, pH 6). For treatment with MeJA, 100 µl of 5 mM MeJA in 50% (v/v) EtOH were distributed on the lid of the Petri dishes, which were consecutively sealed with Parafilm. Control plates were prepared with 50% EtOH. For the analysis of starvation and autophagy, the plants were cultivated on half-strength MS plates without sucrose under short-day conditions at 21 °C. Plates with 8-day-old seedlings were wrapped in aluminum foil and incubated at 21 °C for 8 days.

Other plant material was collected around the University of Konstanz or was purchased in a garden store. Seeds of alfalfa, broccoli and rocket were surface sterilized as above and germinated on filter discs soaked in distilled water.

Confocal microscopy

Protoplasts were isolated from leaves of 2-ODD-C23:GFP expressing and WT plants by overnight incubation in protoplast medium (0.45 M sorbitol, ½ strength MS salt mixture) supplemented with 10 mg ml^{-1} cellulase and 2.5 mg ml^{-1} macerozyme. Spectral images were recorded with a Zeiss LSM880 with a 63x water immersion lens. The samples were excited at 488 nm and images were recorded with 20 spectral channels (9 nm bandwidth) between 490 and 668 nm. A chlorophyll spectrum was obtained from WT protoplasts and a GFP spectrum from an epidermis protoplast that did not contain chloroplasts. Linear unmixing with background subtraction was performed with the ZEN software (Zeiss). Channel overlay, false coloring and adjustment to identical gain, offset and contrast settings were performed in ImageJ and Adobe Photoshop.

Metabolite Analyses

E. coli cultures were lysed by ultrasonication prior to or after the addition of a 20-fold excess of MeOH spiked with 10 µM $^{13}C^{15}N$-guanidine (Sigma-Aldrich 607312). Plant samples were homogenized at -80 °C in a TissueLyser (Qiagen) and resupendend in a 10-fold excess of 80% (w/v) MeOH containing 10 µM $^{13}C^{15}N$-guanidine and 20 µM $^{13}C^{15}N$-arginine (Cortectnet CCN250P). After ultrasonication for 5 min, the suspension was centrifuged for 10 min at maximum speed in a tabletop centrifuge and the supernatant was used directly for metabolite quantification.

Metabolite concentrations in the samples were detemined by high performance liquid chromatography coupled with mass spectroscopy on a LCMS-2020 Single Quadrupole mass spectrometer (Shimadzu). 2 µL sample volume was injected into a Nucleodur HILIC column (250 mm * 2 mm, 3 µm particle size, Macherey-Nagel). Metabolites were eluted at 20 °C with an acetonitrile gradient (90% (v/v) to 60% during 6 min, to 45% in 1 min, constant for 2.5 min, back to 90% in 1.5 min) in 10 mM ammonium formate, 0.2% (v/v) formic acid at a flow rate of 0.15 ml min^{-1}. The separated compounds were analyzed by single ion monitoring (SIM) for positively (and negatively when appropriate) charged ions. Quantification of guanidine, pipecolate and aminoadipate was performed by calibrating peak areas with pure standards and by normalization to the added $^{13}C^{15}N$-guanidine. Homoarginine was quantified by calibrating the peak areas with a pure standard and by normalization to the added $^{13}C^{15}N$-arginine.

Acknowledgments

J.S.H. acknowledges the ERC CoG project 681777 “RiboDisc” for financial support. We thank Astrid Joachimi, Dmitry Galetskiy, and Janine Dietrich for technical assistanceas well as Nicolai Müller and Dieter Spiteller for help with metabolite detection. Additionally, we thank Svetlana Boycheva Woltering for help with autophagy assays as well as Martin Stöckl and the Bioimaging Centre of the University of Konstanz for assistance with confocal microscopy and image processing. We are grateful to Erika Isono and the team of gardeners of the University of Konstanz for access to plant cultivation facilities and plant care.

Author Contributions:

D.F., M.S. and J.S.H. conceived the project. D.F., M.S., and G.F. performed recombinant enzyme expression, purification, and activity assays. D.F. generated and characterized transgenic plants and mutants. D.F. and J.S.H. wrote the manuscript with input from all authors. D.F. and G.F. prepared figures. The manuscript was reviewed and approved by all coauthors.

Competing Interest Statement:

All authors declare the absence of any competing interests.

References

Adams, E., & Frank, L. (1980). Metabolism of proline and the hydroxyprolines. *Annual Review of Biochemistry*, *49*(1), 1005-1061. https://doi.org/10.1146/annurev.bi.49.070180.005041

Arruda, P., & Barreto, P. (2020). Lysine catabolism through the saccharopine pathway: Enzymes and intermediates involved in plant responses to abiotic and biotic stress. *Frontiers in Plant Science*, *11*, 587. https://doi.org/10.3389/fpls.2020.00587

Arruda, P., Kemper, E. L., Papes, F., & Leite, A. (2000). Regulation of lysine catabolism in higher plants. *Trends in Plant Science*, *5*(8), 324-330. https://doi.org/https://doi.org/10.1016/S1360-1385(00)01688-5

Bell, E. A. (1962). α,γ-diaminobutyric acid in Seeds of twelve species of *Lathyrus* and identification of a new natural amino-acid, L-homoarginine, in seeds of other species toxic to man and domestic animals. *Nature*, *193*, 1078-1079.

Bell, E. A. (1980). The non-protein amino acids of higher plants. *Endeavour*, *4*(3), 102-107. https://doi.org/https://doi.org/10.1016/0160-9327(80)90056-3

Bell, E. A. (2003). Nonprotein amino acids of plants: Significance in medicine, nutrition, and agriculture. *Journal of Agricultural and Food Chemistry*, *51*(10), 2854-2865. https://doi.org/10.1021/jf020880w

Bénech, E., & Kutscher, F. (1901). Die Oxydationsprodukte des Arginins. *Hoppe-Seyler´s Zeitschrift für Physiologische Chemie*, *32*(3-4), 278-280. https://doi.org/10.1515/bchm2.1901.32.3-4.278

Bouchereau, J., & Schiff, M. (2020). Inherited disorders of lysine metabolism: A review. *Journal of Nutrition*, *150*(Supplement_1), 2556S-2560S. https://doi.org/10.1093/jn/nxaa112

Brocker, C., Vasiliou, M., Carpenter, S., Carpenter, C., Zhang, Y., Wang, X., Kotchoni, S. O., Wood, A. J., Kirch, H. H., Kopečný, D., Nebert, D. W., & Vasiliou, V. (2013). Aldehyde dehydrogenase (ALDH) superfamily in plants: gene nomenclature and comparative genomics. *Planta*, *237*(1), 189-210. https://doi.org/10.1007/s00425-012-1749-0

Byeon, Y., & Back, K. (2015). Molecular cloning of melatonin 2-hydroxylase responsible for 2-hydroxymelatonin production in rice (*Oryza sativa*). *Journal of Pineal Research*, *58*(3), 343-351. https://doi.org/10.1111/jpi.12220

Caarls, L., Elberse, J., Awwanah, M., Ludwig, N. R., de Vries, M., Zeilmaker, T., Van Wees, S. C. M., Schuurink, R. C., & Van den Ackerveken, G. (2017). Arabidopsis JASMONATE-INDUCED OXYGENASES down-regulate plant immunity by hydroxylation and inactivation of the hormone jasmonic acid. *Proc Natl Acad Sci U S A*, *114*(24), 6388-6393. https://doi.org/10.1073/pnas.1701101114

Choe, C. U., Atzler, D., Wild, P. S., Carter, A. M., Böger, R. H., Ojeda, F., Simova, O., Stockebrand, M., Lackner, K., Nabuurs, C., Marescau, B., Streichert, T., Müller, C., Lüneburg, N., De Deyn, P. P., Benndorf, R. A., Baldus, S., Gerloff, C., Blankenberg, S., . . . Schwedhelm, E. (2013). Homoarginine levels are regulated by L-arginine:glycine amidinotransferase and affect stroke outcome: results from human and murine studies. *Circulation*, *128*(13), 1451-1461. https://doi.org/10.1161/circulationaha.112.000580

Clough, S. J., & Bent, A. F. (1998). Floral dip: a simplified method for *Agrobacterium*-mediated transformation of *Arabidopsis thaliana*. *Plant Journal*, *16*(6), 735-743. https://doi.org/10.1046/j.1365-313x.1998.00343.x

de La Fuente, J. L., Rumbero, A., Martín, J. F., & Liras, P. (1997). Δ-1-piperideine-6-carboxylate dehydrogenase, a new enzyme that forms alpha-aminoadipate in *Streptomyces clavuligerus* and other cephamycin C-producing actinomycetes. *Biochemical Journal*, *327*(1), 59-64. https://pubmed.ncbi.nlm.nih.gov/9355735/

Dunham, N. P., Chang, W.-C., Mitchell, A. J., Martinie, R. J., Zhang, B., Bergman, J. A., Rajakovich, L. J., Wang, B., Silakov, A., Krebs, C., Boal, A. K., & Bollinger, J. M. (2018). Two distinct mechanisms for C–C desaturation by iron(II)- and 2-(oxo)glutarate-dependent oxygenases: Importance of α-heteroatom assistance. *Journal of the American Chemical Society*, *140*(23), 7116-7126. https://doi.org/10.1021/jacs.8b01933

Farrow, S. C., & Facchini, P. J. (2014). Functional diversity of 2-oxoglutarate/Fe(II)-dependent dioxygenases in plant metabolism [Review]. *Frontiers in Plant Science*, *5*. https://doi.org/10.3389/fpls.2014.00524

Forlani, G., Bertazzini, M., Zarattini, M., Funck, D., Ruszkowski, M., & Nocek, B. (2015). Functional properties and structural characterization of rice delta(1)-pyrroline-5-carboxylate reductase. *Frontiers in Plant Science*, *6*, 565. https://doi.org/10.3389/fpls.2015.00565

Forlani, G., Scainelli, D., & Nielsen, E. (1997). Δ^1-Pyrroline-5-carboxylate dehydrogenase from cultured cells of potato (purification and properties). *Plant Physiology*, *113*(4), 1413-1418. https://doi.org/10.1104/pp.113.4.1413

Forlani, G., Trovato, M., Funck, D., & Signorelli, S. (2019). Regulation of proline accumulation and its molecular and physiological functions in stress defence. In M. A. Hossain, V. Kumar, D. J. Burritt, M. Fujita, & P. S. A. Mäkelä (Eds.), *Osmoprotectant-Mediated Abiotic Stress Tolerance in Plants: Recent Advances and Future Perspectives* (pp. 73-97). Springer International Publishing. https://doi.org/10.1007/978-3-030-27423-8_3

Fothergill, J. C., & Guest, J. R. (1977). Catabolism of L-lysine by *Pseudomonas aeruginosa*. *J Gen Microbiol*, *99*(1), 139-155. https://doi.org/10.1099/00221287-99-1-139

Fujii, T., Mukaihara, M., Agematu, H., & Tsunekawa, H. (2002). Biotransformation of L-lysine to L-pipecolic acid catalyzed by L-lysine 6-aminotransferase and pyrroline-5-carboxylate reductase. *Biosci Biotechnol Biochem*, *66*(3), 622-627. https://doi.org/10.1271/bbb.66.622

Fujiki, Y., Yoshikawa, Y., Sato, T., Inada, N., Ito, M., Nishida, I., & Watanabe, A. (2001). Dark-inducible genes from *Arabidopsis thaliana* are associated with leaf senescence and repressed by sugars. *Physiologia Plantarum*, *111*(3), 345-352. https://doi.org/https://doi.org/10.1034/j.1399-3054.2001.1110312.x

Fukuda, H., Ogawa, T., Tazaki, M., Nagahama, K., Fujiil, T., Tanase, S., & Morino, Y. (1992). Two reactions are simultaneously catalyzed by a single enzyme: The arginine-dependent simultaneous formation of two products, ethylene and succinate, from 2-oxoglutarate by an enzyme from *Pseudomonas syringae*. *Biochemical and Biophysical Research Communications*, *188*(2), 483–489. https://doi.org/10.1016/0006-291x(92)91081-z

Funck, D., Sinn, M., Fleming, J. R., Stanoppi, M., Dietrich, J., Lopez-Igual, R., Mayans, O., & Hartig, J. S. (2022). Discovery of a Ni^{2+}-dependent guanidine hydrolase in bacteria. *Nature*. https://doi.org/10.1038/s41586-022-04490-x

Funck, D., Winter, G., Baumgarten, L., & Forlani, G. (2012). Requirement of proline synthesis during Arabidopsis reproductive development. *BMC Plant Biology*, *12*, 191. https://doi.org/10.1186/1471-2229-12-191

Gadjev, I., Vanderauwera, S., Gechev, T. S., Laloi, C., Minkov, I. N., Shulaev, V., Apel, K., Inzé, D., Mittler, R., & Van Breusegem, F. (2006). Transcriptomic footprints disclose specificity of reactive oxygen species signaling in Arabidopsis. *Plant Physiology*, *141*(2), 436-445. https://doi.org/10.1104/pp.106.078717

Gil-Monreal, M., Zabalza, A., Missihoun, T. D., Dormann, P., Bartels, D., & Royuela, M. (2017). Induction of the PDH bypass and upregulation of the ALDH7B4 in plants treated with herbicides inhibiting amino acid biosynthesis. *Plant Science*, *264*, 16-28. https://doi.org/10.1016/j.plantsci.2017.08.003

Goncalves-Butruille, M., Szajner, P., Torigoi, E., Leite, A., & Arruda, P. (1996). Purification and characterization of the bifunctional enzyme lysine-ketoglutarate reductase-saccharopine dehydrogenase from maize. *Plant Physiology*, *110*(3), 765-771. https://doi.org/10.1104/pp.110.3.765

Grefen, C., Donald, N., Hashimoto, K., Kudla, J., Schumacher, K., & Blatt, M. R. (2010). A ubiquitin-10 promoter-based vector set for fluorescent protein tagging facilitates temporal stability and native protein distribution in transient and stable expression studies. *Plant Journal*, *64*(2), 355-365. https://doi.org/10.1111/j.1365-313X.2010.04322.x

Griffiths, G. (2020). Jasmonates: biosynthesis, perception and signal transduction. *Essays Biochem*, *64*(3), 501-512. https://doi.org/10.1042/ebc20190085

Hausinger, R. P. (2015). Biochemical diversity of 2-oxoglutarate-dependent oxygenases. In C. J. Schofield & R. P. Hausinger (Eds.), *2-Oxoglutarate-Dependent Oxygenases* (pp. 1-58). The Royal Society of Chemistry. https://doi.org/10.1039/9781782621959-00001

Hauth, F., Buck, H., Stanoppi, M., & Hartig, J. S. (2022). Canavanine utilization via homoserine and hydroxyguanidine by a PLP-dependent gamma-lyase in *Pseudomonadaceae* and *Rhizobiales*. *RSC Chem Biol*, *3*(10), 1240-1250. https://doi.org/10.1039/d2cb00128d

Herr, C. Q., & Hausinger, R. P. (2018). Amazing diversity in biochemical roles of Fe(II)/2-oxoglutarate oxygenases. *Trends in Biochemical Sciences*, *43*(7), 517-532. https://doi.org/10.1016/j.tibs.2018.04.002

Kawai, Y., Ono, E., & Mizutani, M. (2014). Evolution and diversity of the 2-oxoglutarate-dependent dioxygenase superfamily in plants. *Plant Journal*, *78*(2), 328-343. https://doi.org/10.1111/tpj.12479

Koch, V., Gruenewald, L. D., Gruber-Rouh, T., Eichler, K., Leistner, D. M., Mahmoudi, S., Booz, C., Bernatz, S., D'Angelo, T., Albrecht, M. H., Alizadeh, L. S., Nour-Eldin, N. A., Scholtz, J. E., Yel, I., Vogl, T. J., März, W., Hardt, S. E., & Martin, S. S. (2022). Homoarginine in the cardiovascular system: Pathophysiology and recent developments. *Fundamental & Clinical Pharmacology*, *36*, 1-11. https://doi.org/10.1111/fcp.12858

Končitíková, R., Vigouroux, A., Kopečná, M., Andree, T., Bartoš, J., Šebela, M., Moréra, S., & Kopečný, D. (2015). Role and structural characterization of plant aldehyde dehydrogenases from family 2 and family 7. *Biochemical Journal*, *468*(1), 109-123. https://doi.org/10.1042/BJ20150009

Kotchoni, S. O., Kuhns, C., Ditzer, A., Kirch, H. H., & Bartels, D. (2006). Over-expression of different aldehyde dehydrogenase genes in *Arabidopsis thaliana* confers tolerance to abiotic stress and protects plants against lipid peroxidation and oxidative stress. *Plant Cell Environ*, *29*(6), 1033-1048. https://doi.org/10.1111/j.1365-3040.2005.01458.x

Lambein, F., Khan, J. K., & Kuo, Y.-H. (1992). Free amino acids and toxins in *Lathyrus sativus* seedlings. *Planta Med*, *58*(04), 380-381. https://doi.org/10.1055/s-2006-961491

Lambein, F., Travella, S., Kuo, Y. H., Van Montagu, M., & Heijde, M. (2019). Grass pea (*Lathyrus sativus* L.): orphan crop, nutraceutical or just plain food? *Planta*, *250*(3), 821-838. https://doi.org/10.1007/s00425-018-03084-0

Lenkeit, F., Eckert, I., Hartig, J. S., & Weinberg, Z. (2020). Discovery and characterization of a fourth class of guanidine riboswitches. *Nucleic Acids Research*, *48*(22), 12889-12899. https://doi.org/10.1093/nar/gkaa1102

León, J., & Costa-Broseta, Á. (2020). Present knowledge and controversies, deficiencies, and misconceptions on nitric oxide synthesis, sensing, and signaling in plants. *Plant Cell Environ*, *43*(1). https://doi.org/10.1111/pce.13617

Magen, S., Seybold, H., Laloum, D., & Avin-Wittenberg, T. (2022). Metabolism and autophagy in plants - a perfect match. *FEBS Letters*, *596*(17), 2133-2151. https://doi.org/https://doi.org/10.1002/1873-3468.14359

Marsden, K. A., Scowen, M., Hill, P. W., Jones, D. L., & Chadwick, D. R. (2015). Plant acquisition and metabolism of the synthetic nitrification inhibitor dicyandiamide and naturally-occurring guanidine from agricultural soils. *Plant and Soil*, *395*(1), 201-214. https://doi.org/10.1007/s11104-015-2549-7

Martinez, S., Fellner, M., Herr, C. Q., Ritchie, A., Hu, J., & Hausinger, R. P. (2017). Structures and mechanisms of the non-heme Fe(II)- and 2-oxoglutarate-dependent ethylene-forming enzyme: Substrate binding creates a twist. *Journal of the American Chemical Society*, *139*(34), 11980-11988. https://doi.org/10.1021/jacs.7b06186

Martinez, S., & Hausinger, R. P. (2016). Biochemical and Spectroscopic Characterization of the Non-Heme Fe(II)- and 2-Oxoglutarate-Dependent Ethylene-Forming Enzyme from Pseudomonas syringae pv. phaseolicola PK2. *Biochemistry*, *55*(43), 5989-5999. https://doi.org/10.1021/acs.biochem.6b00890

Moreira, E., Coimbra, S., & Melo, P. (2022). Glutamine synthetase: an unlikely case of functional redundancy in Arabidopsis thaliana. *Plant Biol (Stuttg)*, *24*(5), 713-720. https://doi.org/10.1111/plb.13408

Nelson, J. W., Atilho, R. M., Sherlock, M. E., Stockbridge, R. B., & Breaker, R. R. (2017). Metabolism of free guanidine in bacteria is regulated by a widespread riboswitch class. *Molecular Cell*, *65*(2), 220–230. https://doi.org/10.1016/j.molcel.2016.11.019

Precision Reports. (2021). *Global guanidine market research report 2021*. Retrieved 2023-02-23 from https://www.precisionreports.co/global-guanidine-market-17253362

Prescott, A. G., & John, P. (1996). Dioxygenases: Molecular structure and role in plant metabolism. *Annual Review of Plant Physiology and Plant Molecular Biology*, *47*, 245-271. https://doi.org/10.1146/annurev.arplant.47.1.245

Rao, S. L. N., Ramachandran, L. K., & Adiga, P. R. (1963). The isolation and characterization of L-homoarginine from seeds of *Lathyrus sativus*. *Biochemistry*, *2*(2), 298-300. https://doi.org/10.1021/bi00902a019

Salvail, H., Balaji, A., Yu, D., Roth, A., & Breaker, R. R. (2020). Biochemical validation of a fourth guanidine riboswitch class in bacteria. *Biochemistry*, *59*(49), 4654-4662. https://doi.org/10.1021/acs.biochem.0c00793

Schneider, N. O., Tassoulas, L. J., Zeng, D., Laseke, A. J., Reiter, N. J., Wackett, L. P., & Maurice, M. S. (2020). Solving the conundrum: Widespread proteins annotated for urea metabolism in bacteria are carboxyguanidine deiminases mediating nitrogen assimilation from guanidine. *Biochemistry*, *59*(35), 3258-3270. https://doi.org/10.1021/acs.biochem.0c00537

Schulze, E. (1893). Ueber einige stickstoffhaltige Bestandtheile der Keimlinge von *Vicia sativa*. *Zeitschrift für Physiologische Chemie*, *17*, 193-216. https://vlp.mpiwg-berlin.mpg.de/library/data/lit16884?

Sharma, I., Kashyap, S., & Agarwala, N. (2023). Biotic stress-induced changes in root exudation confer plant stress tolerance by altering rhizospheric microbial community. *Frontiers in Plant Science*, *14*, 1132824. https://doi.org/10.3389/fpls.2023.1132824

Shen, Y., Zhang, Y., Yang, C., Lan, Y., Liu, L., Liu, S., Chen, Z., Ren, G., & Wan, J. (2012). Mutation of OsALDH7 causes a yellow-colored endosperm associated with accumulation of oryzamutaic acid A in rice. *Planta*, *235*(2), 433-441. https://doi.org/10.1007/s00425-011-1477-x

Sherlock, M. E., & Breaker, R. R. (2017). Biochemical Validation of a Third Guanidine Riboswitch Class in Bacteria. *Biochemistry*, *56*(2), 359–363. https://doi.org/10.1021/acs.biochem.6b01271

Sherlock, M. E., Malkowski, S. N., & Breaker, R. R. (2017). Biochemical Validation of a Second Guanidine Riboswitch Class in Bacteria. *Biochemistry*, *56*(2), 352–358. https://doi.org/10.1021/acs.biochem.6b01270

Shin, J. H., Kim, S. R., & An, G. (2009). Rice aldehyde dehydrogenase7 is needed for seed maturation and viability. *Plant Physiology*, *149*(2), 905-915. https://doi.org/10.1104/pp.108.130716

Sinn, M., Hauth, F., Lenkeit, F., Weinberg, Z., & Hartig, J. S. (2021). Widespread bacterial utilization of guanidine as nitrogen source. *Molecular Microbiology*. https://doi.org/10.1111/mmi.14702

Srivenugopal, K. S., & Adiga, P. R. (1980). Partial purification and properties of a transamidinase from *Lathyrus sativus* seedlings. Involvement in homoarginine metabolism and amine interconversions. *Biochemical Journal*, *189*(3), 553-560. https://doi.org/10.1042/bj1890553

Strecker, A. (1861). Untersuchungen über die chemischen Beziehungen zwischen Guanin, Xanthin, Theobromin, Caffeïn und Kreatinin. *Justus Liebigs Annalen der Chemie*, *118*(2), 151-177. https://doi.org/10.1002/jlac.18611180203

Struys, E. A., Jansen, E. E. W., & Salomons, G. S. (2014). Human pyrroline-5-carboxylate reductase (PYCR1) acts on Δ^1-piperideine-6-carboxylate generating L-pipecolic acid. *Journal of Inherited Metabolic Disease*, *37*(3), 327-332. https://doi.org/10.1007/s10545-013-9673-4

Sulser, H., & Sager, F. (1976). Identification of uncommon amino acids in the lentil seed (*Lens culinaris* Med.). *Experientia*, *32*(4), 422-423. https://doi.org/10.1007/BF01920772

Tassoulas, L. J., Robinson, A., Martinez-Vaz, B., Aukema, K. G., & Wackett, L. P. (2021). Filling in the gaps in metformin biodegradation: a new enzyme and a metabolic pathway for guanylurea. *Applied and Environmental Microbiology*, *87*(11). https://doi.org/10.1128/AEM.03003-20

Trovato, M., Forlani, G., Signorelli, S., & Funck, D. (2019). Proline metabolism and its functions in development and stress tolerance. In M. A. Hossain, V. Kumar, D. J. Burritt, M. Fujita, & P. S. A. Mäkelä (Eds.), *Osmoprotectant-Mediated Abiotic Stress Tolerance in Plants: Recent Advances and Future Perspectives* (pp. 41-72). Springer International Publishing. https://doi.org/10.1007/978-3-030-27423-8_2

van Karnebeek, C. D. M., Tiebout, S. A., Niermeijer, J., Poll-The, B. T., Ghani, A., Coughlin, C. R., Van Hove, J. L. K., Richter, J. W., Christen, H. J., Gallagher, R., Hartmann, H., & Stoclder-Ipsiroglu, S. (2016). Pyridoxine-dependent epilepsy: An expanding clinical spectrum [Review]. *Pediatric Neurology*, *59*, 6-12. https://doi.org/10.1016/j.pediatrneurol.2015.12.013

Wang, B., Xu, Y., Wang, X., Yuan, J. S., Johnson, C. H., Young, J. D., & Yu, J. P. (2021). A guanidine-degrading enzyme controls genomic stability of ethylene-producing cyanobacteria [Article]. *Nature Communications*, *12*(1), 13, Article 5150. https://doi.org/10.1038/s41467-021-25369-x

Wang, Z. P., Xing, H. L., Dong, L., Zhang, H. Y., Han, C. Y., Wang, X. C., & Chen, Q. J. (2015). Egg cell-specific promoter-controlled CRISPR/Cas9 efficiently generates homozygous mutants for multiple target genes in Arabidopsis in a single generation. *Genome Biol*, *16*(1), 144. https://doi.org/10.1186/s13059-015-0715-0

Winter, G., Todd, C. D., Trovato, M., Forlani, G., & Funck, D. (2015). Physiological implications of arginine metabolism in plants. *Frontiers in Plant Science*, *6*, 534. https://doi.org/10.3389/fpls.2015.00534

Xue, J., Wang, J., Gong, P., Wu, M., Yang, W., Jiang, S., Wu, Y., Jiang, Y., Zhang, Y., Yuzyuk, T., Li, H., & Yang, Z. (2019). Simultaneous quantification of alpha-aminoadipic semialdehyde, piperideine-6-carboxylate, pipecolic acid and alpha-aminoadipic acid in pyridoxine-dependent epilepsy. *Sci Rep*, *9*(1), 11371. https://doi.org/10.1038/s41598-019-47882-2

Zeier, J. (2021). Metabolic regulation of systemic acquired resistance. *Current Opinion in Plant Biology*, *62*, 102050. https://doi.org/10.1016/j.pbi.2021.102050

Zhang, H., Zhang, F., Yu, Y., Feng, L., Jia, J., Liu, B., Li, B., Guo, H., & Zhai, J. (2020). A comprehensive online database for exploring 20,000 public Arabidopsis RNA-Seq libraries. *Molecular Plant*, *13*(9), 1231-1233. https://doi.org/10.1016/j.molp.2020.08.001

Zhang, Y., Zhao, L., Zhao, J., Li, Y., Wang, J., Guo, R., Gan, S., Liu, C.-J., & Zhang, K. (2017). S5H/DMR6 encodes a salicylic acid 5-hydroxylase that fine-tunes salicylic acid homeostasis. . *Plant Physiology*, *175*(3), 1082-1093. https://doi.org/10.1104/pp.17.00695

Supplementary material

To the manuscript

Guanidine Production by Plant Homoarginine-6-hydroxylases

Dietmar Funck[1*], Malte Sinn[1], Giuseppe Forlani[2], and Jörg S. Hartig[1*]

[1] Department of Chemistry, University of Konstanz, 78457 Konstanz

[2] Department of Life Science and Biotechnology, University of Ferrara, 44121 Ferrara, Italy

* Correspondence: Jörg S. Hartig, Dietmar Funck

Email: joerg.hartig@uni-konstanz.de, dietmar.funck@uni-konstanz.de

The supplementary material comprises:

Figures S1 to S10

Tables S1 to S3

SI References

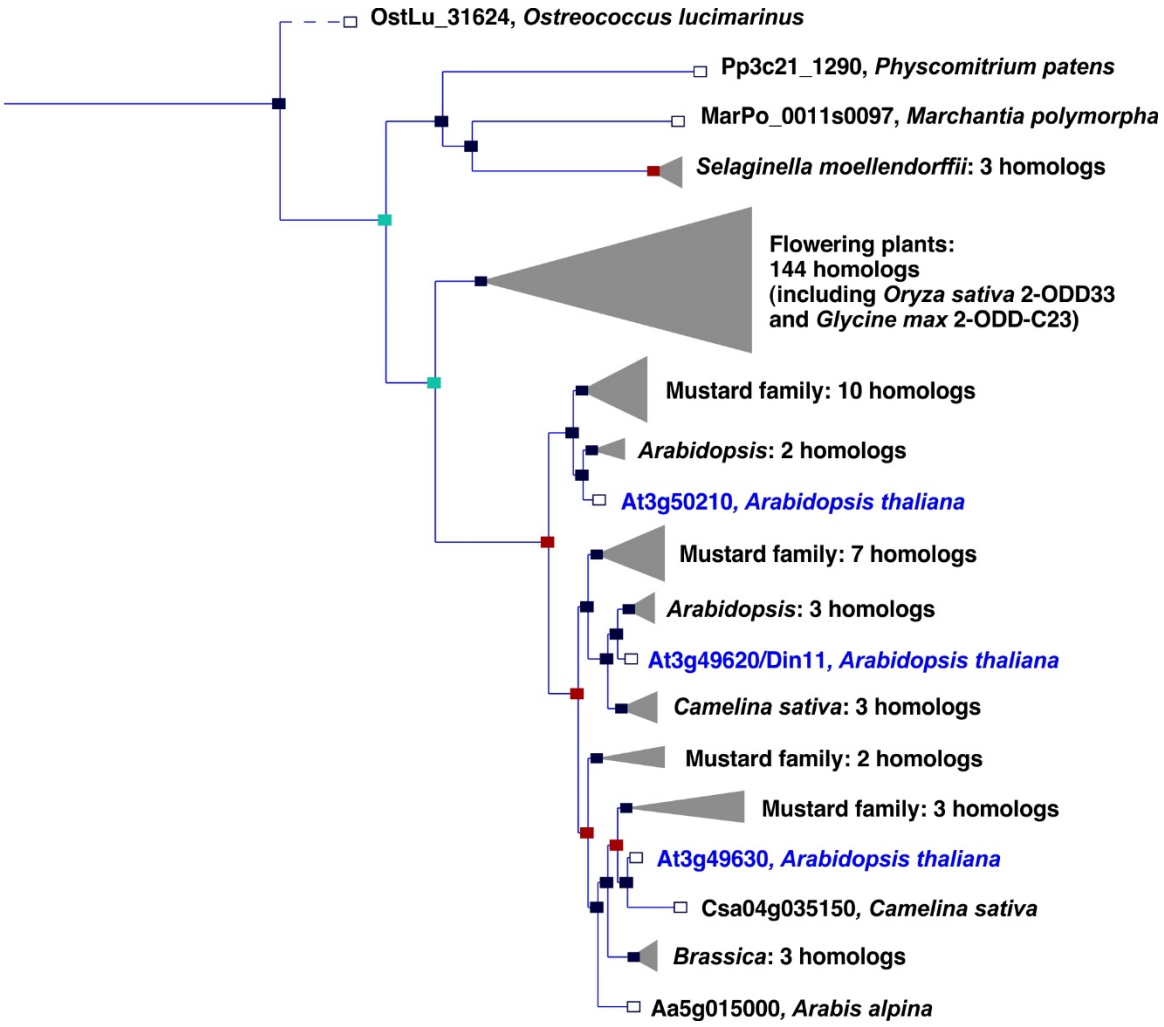

Fig. S1: Phylogeny of the 2-ODD clade C23. Excerpt of the gene tree for *Din11* from EnsemblPlants (https://plants.ensembl.org, accessed Feb. 2023). The length of the horizontal blue lines is proportional to the number of amino acid exchanges except the dashed line, which is shortened by a factor of 10. Blue squares indicate speciation nodes, red squares indicate duplication nodes, green squares indicate ambiguous nodes, and open squares indicate species nodes. Grey triangles indicate collapsed branches. The three 2-ODD-C23 paralogues from *Arabidopsis thaliana* are highlighted by blue lettering.

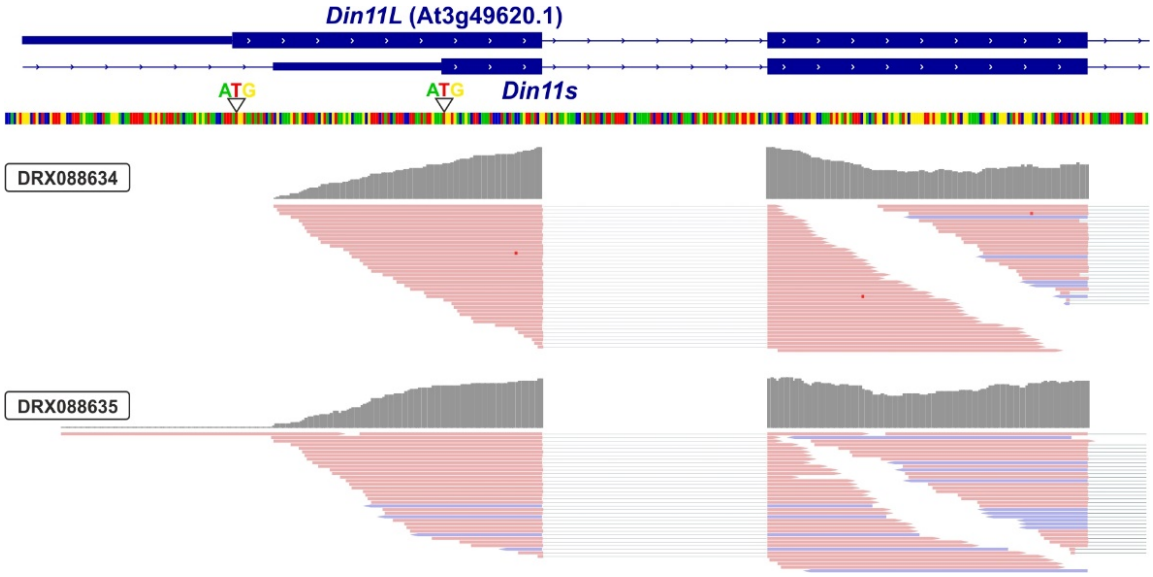

Fig. S2: 3′-UTR of *Din11*. Alignment of RNAseq reads (pink or purple lines) from two independent experiments with the genomic sequence (four-coloured line) of Arabidopsis around the transcription start site of *Din11*. The 5′-end of the annotated *Din11* transcript At3g49620.1/*Din11L* is hardly covered by RNAseq reads, which are much more frequent several basepairs downstream of the annotated start codon. The graphical representation of the RNAseq reads was modified from the Arabidopsis RNAseq database (Zhang et al., 2020).

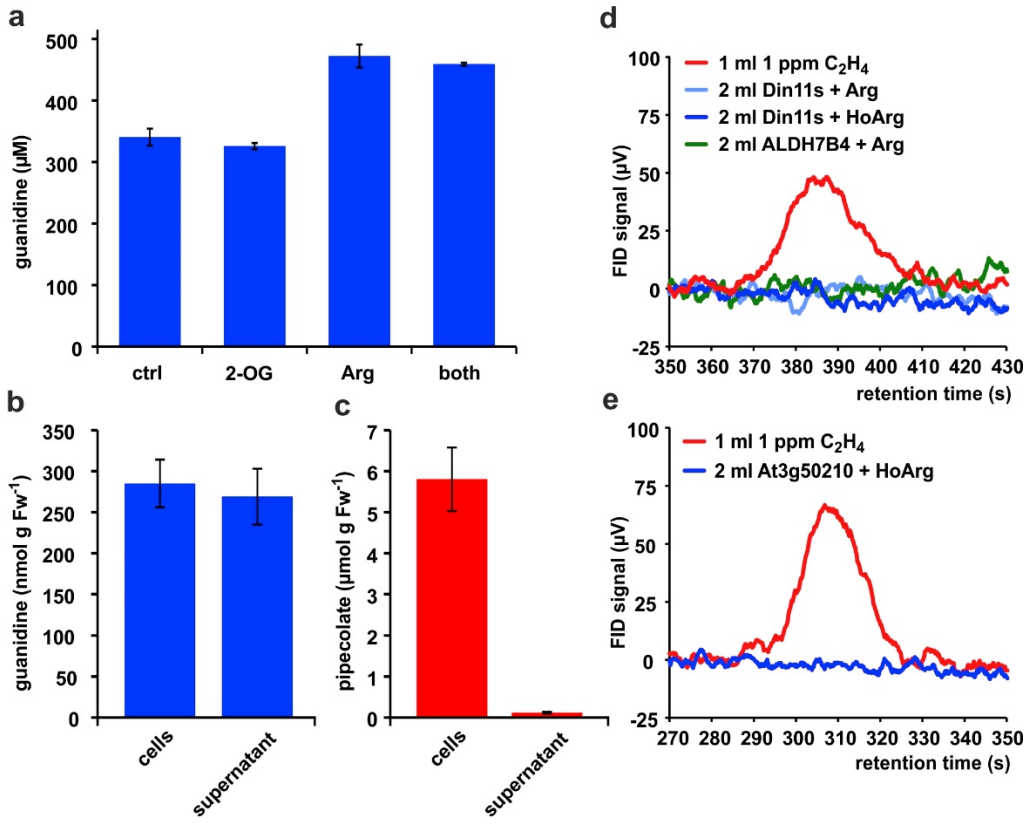

Fig. S3: Distribution of metabolites in *E. coli* cultures. (a) *E. coli* cells expressing Din11s were cultivated over night at 18 °C in medium supplemented with either 5 mM 2-oxoglutarate (2-OG), 5 mM arginine (Arg), or a combination of both. The cultures were diluted with a 20-fold excess of methanol containing 10 µM $^{13}C^{15}N$-labelled guanidine as analytical standard. (b), (c) *E. coli* cells expressing soybean 2-ODD-C23 were grown over night at 18 °C in the presence of 1 mM homoarginine. The cells were harvested by centrifugation and lysed in 20 µl (mg Fw)$^{-1}$ methanol containing 10 µM labelled guanidine. The supernatant was also mixed with a 20-fold excess of methanol with 10 µM labelled guanidine. Guanidine and pipecolate were quantified by LC-MS. The columns are the average ±SD of samples from three independent cultures. The experiments were repeated with consistent results. (d) and (e) Flame ionization detector traces of samples from the headspace of *E. coli* cultures overexpressing either ALDH7B4 (negative control), Din11s, or At3g50210 and supplemented with 5 mM Arg or homoarginine (HoArg) as indicated in the figures. One ml of a 1 ppm C_2H_4 standard or 2 ml of culture headspace were injected into a gas chromatograph (SGI 8610C, SRI Instruments, Los Angeles, CA, United States) equipped with a 3 m Hayesep-D column (60 °C, carrier gas N_2). C_2H_4 was detected with a flame ionization detector (135 °C). The software PeakSimple v4.44 was used to record the chromatograms. The detector output was smoothed by averaging 9 measurements recorded at 5 Hz. Retention times for C_2H_4 shifted over time but were consistent within each set of measurements.

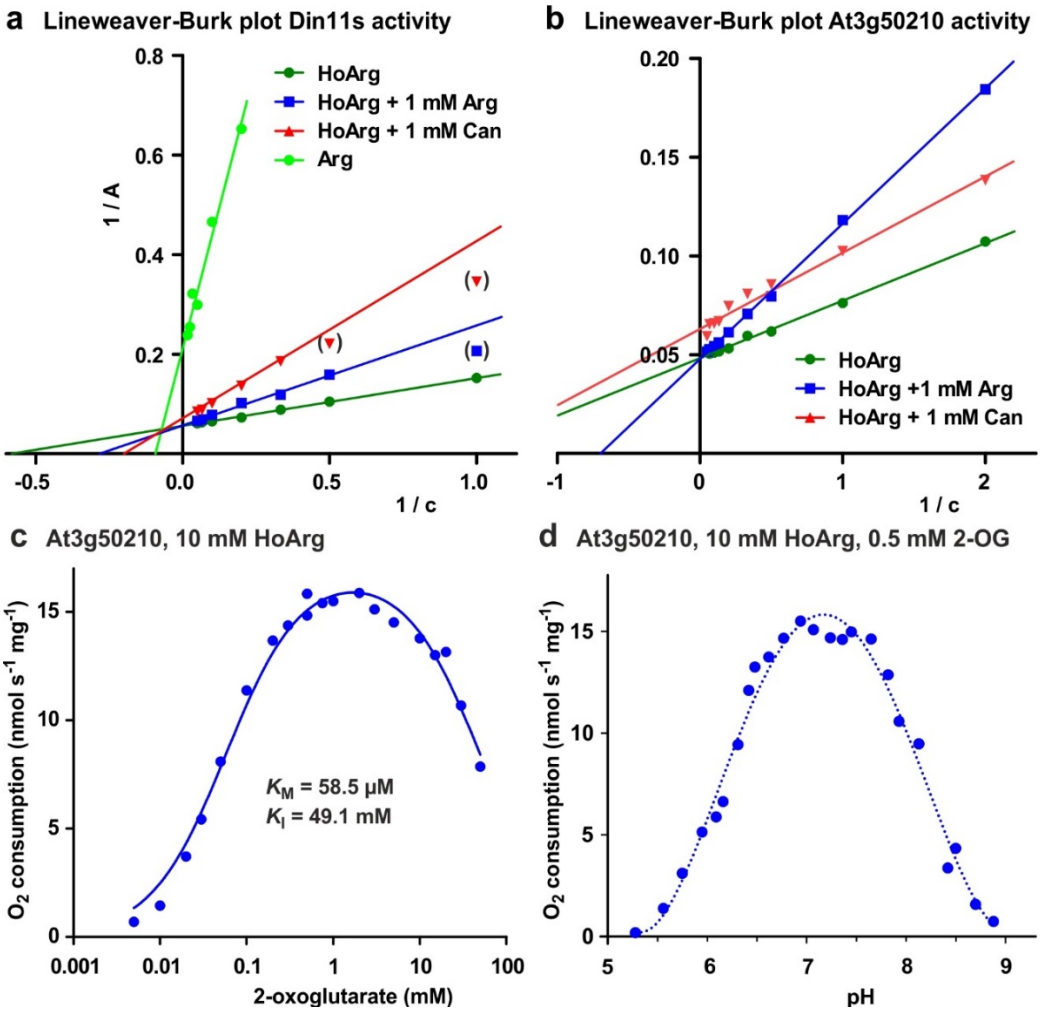

Fig. S4: Biochemical characterization of 2-ODD-C23 isoforms. (a), Lineweaver-Burk plot of the activity data for Din11s from Fig. 2a. Values in brackets are very low activities at low concentrations of homoarginine (HoArg) in presence of 1 mM arginine (Arg) or canavanine (Can) that were excluded from the linear regression. (b), Lineweaver-Burk plot of the activity data for At3g50210 from Fig. 2c. Regression lines intersecting on or very near the Y-axis indicate competitive inhibition. (c) Specific activity of At3g50210 in dependence on the concentration of the co-substrate 2-oxoglutarate was determined at 30 °C. Homoarginine concentration was fixed at 10 mM. The blue line represents the least square fit to the Michaelis-Menten equation with an additional term for substrate inhibition. (d), pH-dependence of the specific activity of At3g50210 in a mixed buffer system with MES, HEPES and CHES. Homoarginine and 2-oxoglutarate (2-OG) concentrations were fixed at 10 mM and 0.5 mM, respectively. The dashed blue line is a polynomic fit with a 4th-order polynomial. Dots represent single measurements and independent enzyme preparations gave consistent results.

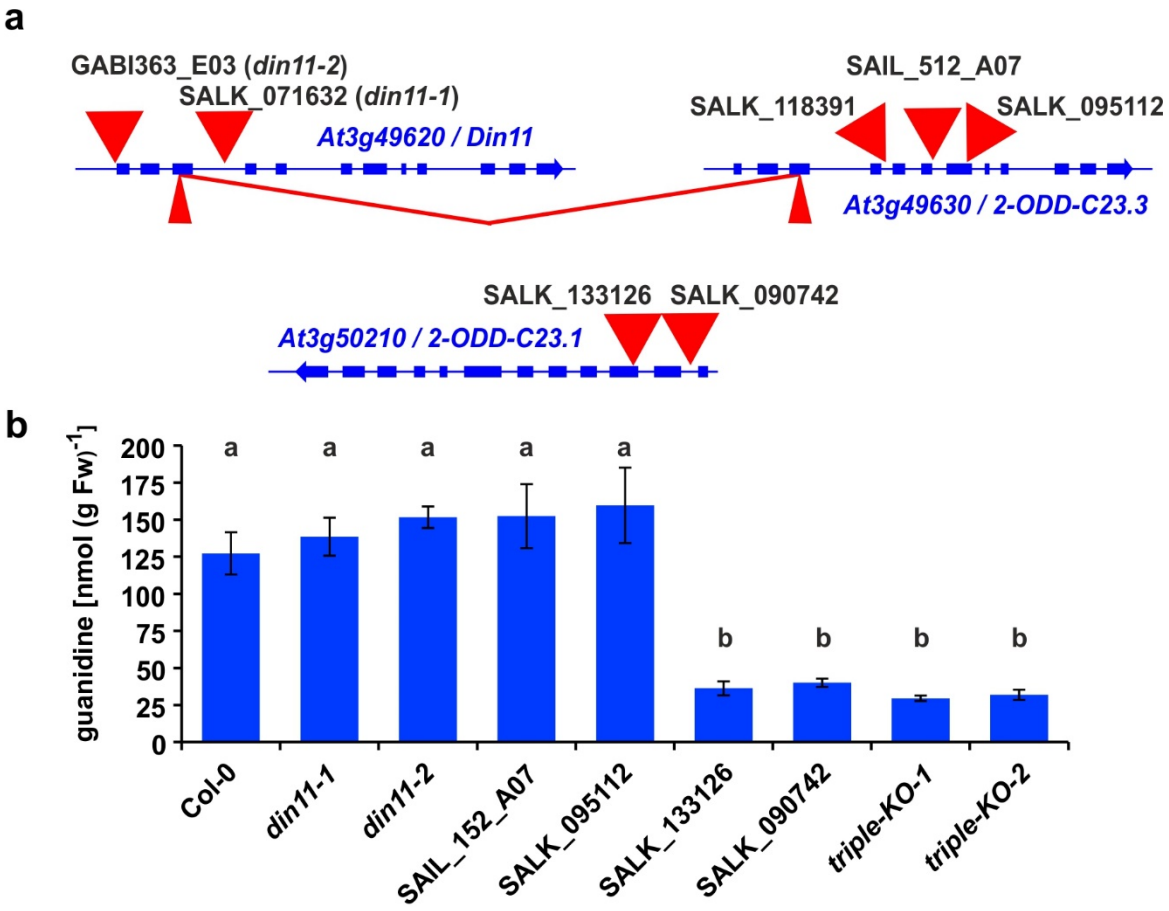

Fig. S5: 2-ODD-C23 mutants in Arabidopsis. (a) Schematic representation of the three genes for 2-ODD-C23 isoforms in Arabidopsis. Thick blue lines represent exons, wide red triangles represent T-DNA insertions, narrow red triangles represent CRISPR/Cas9 target sites. The red lines indicate a fusion event between Din11 and At3g49630, in which the DNA fragment between the two CRISPR/CAs9 target sites was lost. (b) Guanidine content in rosettes of single and triple mutant seedlings cultivated under axenic conditions. The seedlings were cultivated for 9 days under long day conditions on half-strength MS medium supplemented with 2% sucrose. Subsequently, they were transferred for one week to plates supplemented additionally with 0.2 mM homoarginine. Columns represent the average ±SD of N = 4 independent samples. Different letters above the columns indicate significant differences ($p < 0.05$) by one-way ANOVA with Bonnferroni correction for multiple testing.

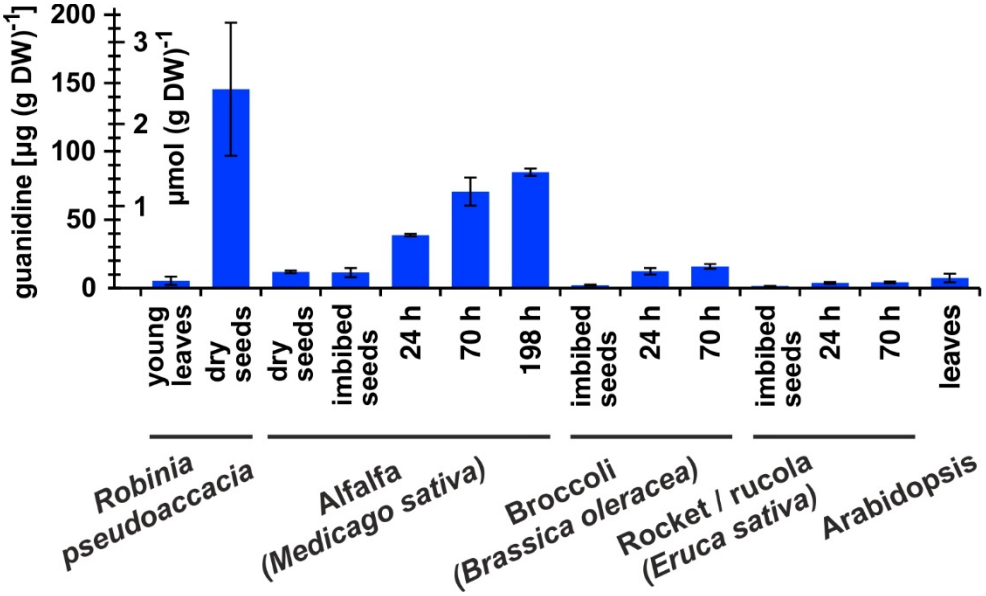

Fig. S6: Guanidine content in various plants. Black locust (*Robinia pseudoaccacia*) and Arabidopsis samples were from soil-grown plants. Seeds were surface-sterilised and germinated on filter paper soaked with ddH_2O for the indicated times. Guanidine was extracted in 80% (v/v) methanol with 10 µM $^{13}C^{15}N$-labelled guanidine as analytical standard and quantified by LC-MS. Columns represent the average ±SD of N = 3 independent samples.

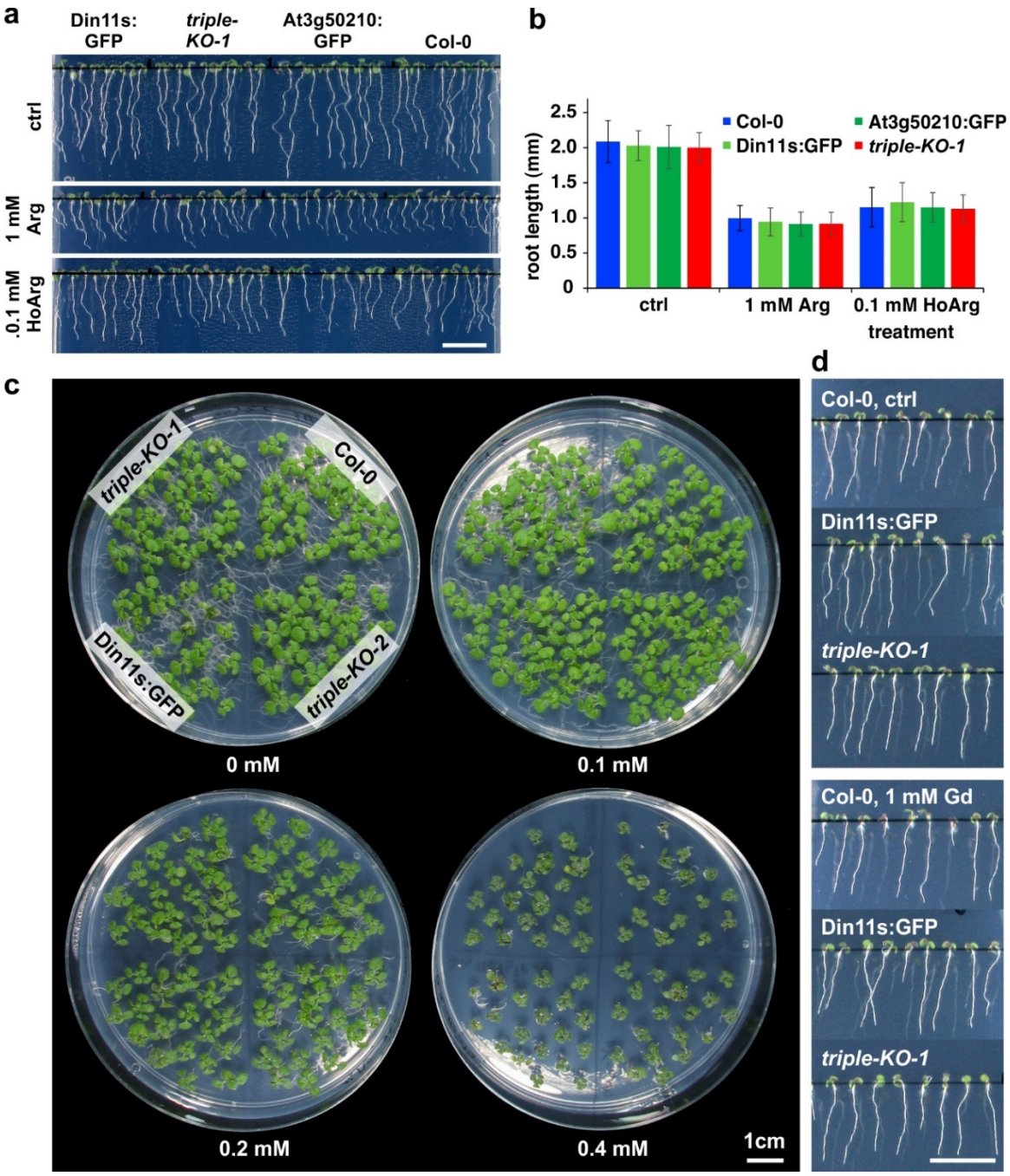

Fig. S7: Growth inhibition by homoarginine. (a), (b) Seedlings of WT Arabidopsis plants (Col-0) and 2-ODD-C23 overexpressors or triple mutants were grown for 6 days under long-day conditions on vertical plates containing half-strength MS medium, supplemented with 2% (w/v) sucrose and either arginine (Arg) or homoarginine (HoArg). Columns in (b) represent the average ±SD of N = 40 seedlings. (c) Two-week old seedlings grown on half-strength MS medium with 2% (w/v) sucrose and the indicated concentration of homoarginine. The positioning of the genotypes is identical on each plate. (d) Seven-day-old seedlings grown on vertical plates without or with 1 mM guanidine (Gd). Scale bars in (a), (c) and (d) are 1 cm.

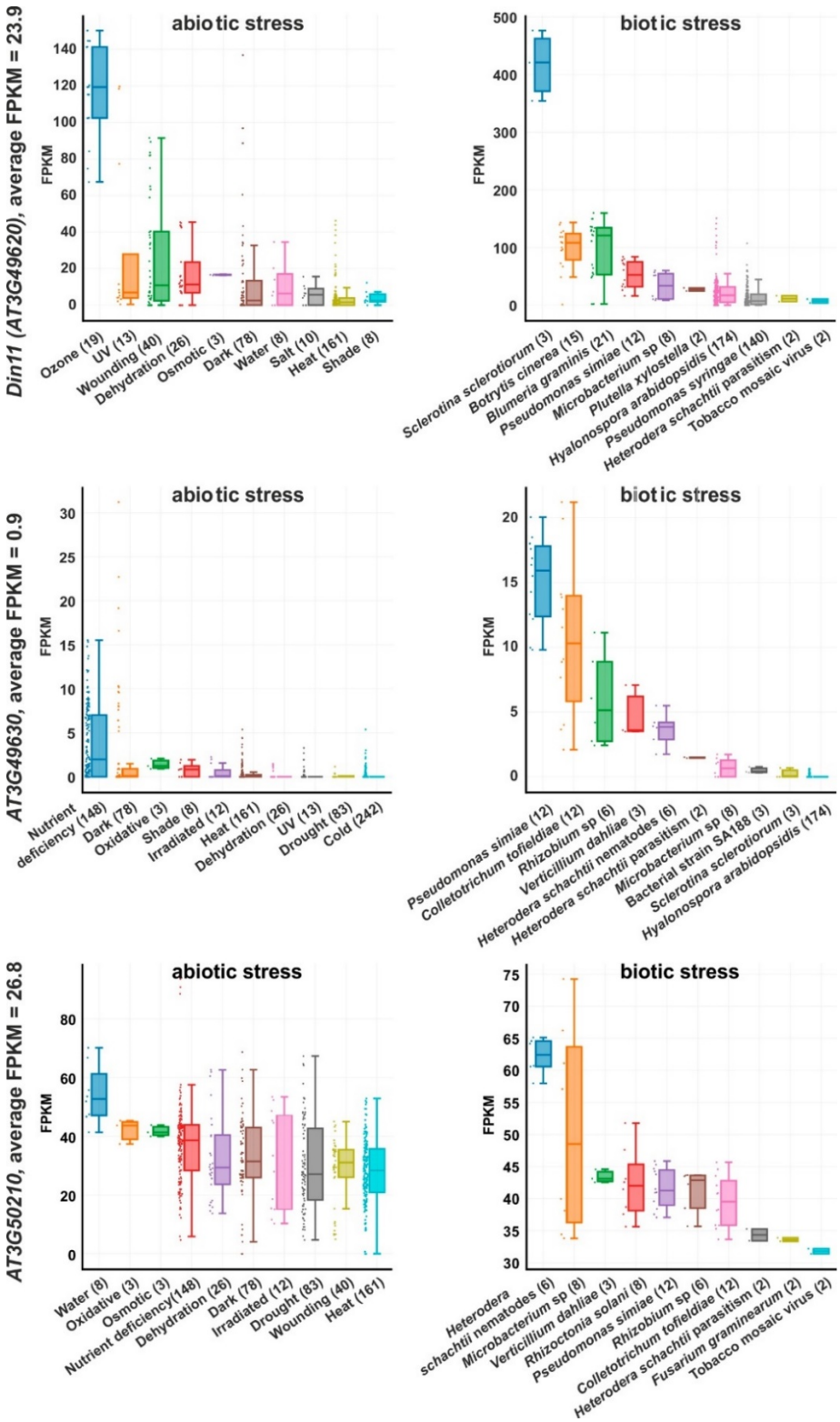

Fig. S8: Expression levels of *2-ODD-C23s* under stress. RNAseq coverage of the three Arabidopsis *2-ODD-C23* isoforms under various abiotic and biotic stress conditions. The data plots were modified from the Arabidopsis RNAseq database (Zhang et al., 2020). Numbers in brackets are the number of samples per treatment. FPKM, Fragments per kilobase of transcript per million mapped reads.

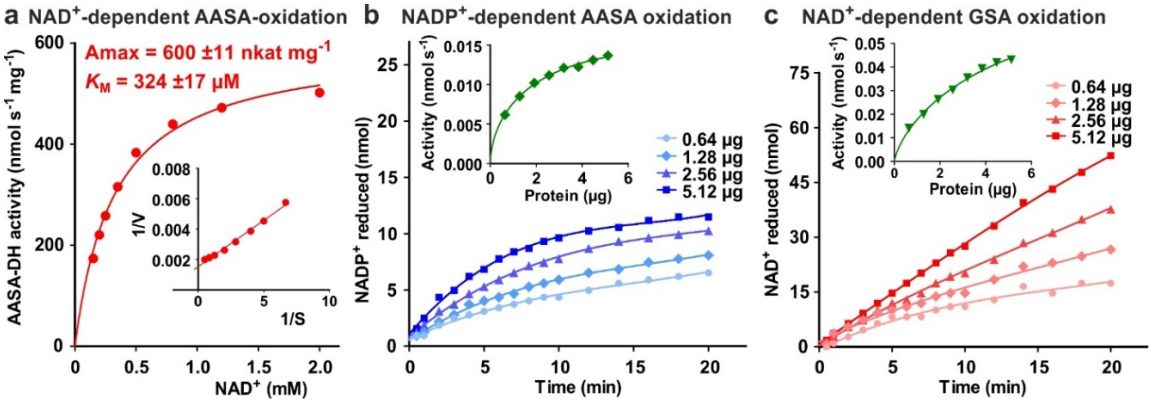

Fig. S9: Characterization of ALDH7B4 (At1g54100). (a) Activity of purified recombinant ALDH7B4 with different concentrations of NAD^+ at 35 °C. AASA/P6C concentration was fixed at 1 mM. K_M and A_{max} values were obtained by nonlinear regression to the Michaelis-Menten equation (red line). The inset shows the Lineweaver-Burk plot of the same data. (b) AASA/P6C-dependent reduction of $NADP^+$ by different amounts of ALDH7B4. Concentrations of both $NADP^+$ and AASA/P6C were 1 mM. (c) GSA/P5C-dependent reduction of NAD^+ by different amounts of ALDH7B4. NAD^+ concentration was 1 mM and DL-GSA/P5C concentration was 2 mM. In b and c, the insets show the initial velocity as a function of the amount of protein in the assay. Data points are the average ±SD of technical triplicates. All experiments were repeated with an independent enzyme preparation.

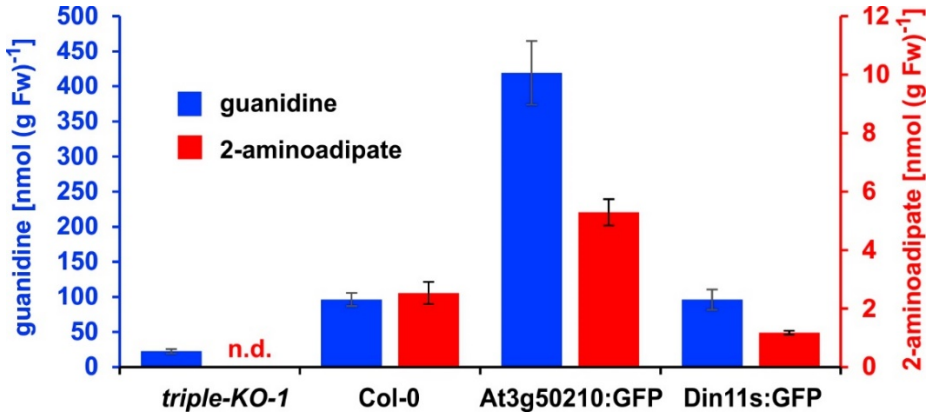

Fig. S10: 2-Aminoadipate content after homoarginine feeding. Arabidopsis seedlings were grown for ten days under long-day conditions on half-strength MS medium supplemented with 2% (w/v) sucrose and 5 mM MES-KOH, pH 5.8 before they were transferred for four days to plates additionally containing 0.2 mM homoarginine. Guanidine and 2-aminoadipate were extracted in 80% (v/v) methanol containing 10 µM $^{13}C^{15}N$-labelled guanidine as analytical standard and quantified by LC-MS. Columns represent the average ±SD of N = 4 independent samples. n.d., not detected. The experiment was repeated with consistent results.

Table S1: Kinetic constants of Arabidopsis 2-ODD-C23 enzymes

	Homoarginine variable, 0.5 mM 2-oxoglutarate		
	Inhibitor (1 mM)	A_{max} (nmol s^{-1} mg^{-1})	K_M (mM)
Din11s	none	13.4 ±3.2	1.9 ±0.3
	Arginine	12.9 ±3.5	3.6 ±0.5
	Canavanine	11.2 ±2.7	5.5 ±1.0
At3g49630	none	5.6 ±1.2	4.6 ±0.2
	Arginine	5.4 ±1.3	4.1 ±0.8
	Canavanine	5.4 ±1.4	4.1 ±0.7
At3g50210	none	20.9 ±1.7	0.78 ±0.15
	Arginine	21.3 ±3.7	1.75 ±0.43
	Canavanine	16.2 ±2.3	0.74 ±0.09

	Arginine variable, 0.5 mM 2-oxoglutarate		2-Oxoglutarate variable, 10 mM homoarginine		
	A_{max} (nmol s^{-1} mg^{-1})	K_M (mM)	A_{max} (nmol s^{-1} mg^{-1})	K_M (µM)	K_I (mM)
Din11s	3.1 ±1.4	6.0 ±5.1	5.2 ±0.9	30.1 ±9.4	17.6 ±9.6
At3g49630	n.d.		3.1 ±0.4	53.8 ±37.1	36.8 ±8.8
At3g50210	n.d.		19.0 ±7.2	69.7 ±23.2	35.3 ±20.1

All data are the average ±SD from 3 to 5 independent enzyme preparations

Table S2: Arabidopsis T-DNA insertion lines used in this study

Line	NASC stock Nr.	Position of T-DNA	Reference
SALK_071632	N571632	3rd intron of *Din11*	(Alonso et al., 2003)
GK-363E06	N434806	1st exon of *Din11L* 5′-UTR of *Din11s*	(Kleinboelting et al., 2012)
SALK_118391	N618391	4th intron of *At3g49630*	(Alonso et al., 2003)
SAIL_512_A07	N821581	6th intron of *At3g49630*	(Sessions et al., 2002)
SALK_095112	N595112	7th exon of *At3g49630*	(Alonso et al., 2003)
SALK_133126	N633126	3rd exon of *At3g50210*	(Alonso et al., 2003)
SALK_098742	N598742	1st intron of *At3g50210*	(Alonso et al., 2003)

Table S3: Sequences of primers used in this study

For cDNA insertion into pET24 (pET) or pENTR (pE)	
DIN11L-pET-f	gtactttcaaggtgctATGGTAATATATCATCGCAAAG
Din11s-pET-f	tgtactttcaaggtgctATGGTGACAGACTTCAAATCC
DIN11-pET-r	gtggtgctcgagtgcccataTTAACTGTTTTCCAC
DIN11L-pE-f	caggctttaaaggaacctATGGTAATATATCATCGCAAAG
DIN11s-pE-f	caggctttaaaggaacctATGGTGACAGACTTCAAATCC
DIN11-pE-r	gaaagctgggtctagataACTGTTTTCCACTAAATTTGC
49630-pET-f	tgtactttcaaggtgctATGGCGACAAACTTCAAATCC
49630-pET-r	ggtggtgctcgagtgctaacaTTAACTGTGTTCCACT
49630-pE-f	caggctttaaaggaaccATGGCGACAAACTTCAAATCC
49630-pE-NS-r	gaaagctgggtctagataACTGTGTTCCACTAAATTTTG
50210-pET-f	tgtactttcaaggtgctATGGCGACGGACTTCAAGTCT
50210-pET-r	ggtggtgctcgagtgccaTTACATAGCAAAGTTGGTC
50210-pE-f	caggctttaaaggaaccatggcgacggacttcaag
50210-pE-NS-r	gaaagctgggtctagatgCATAGCAAAGTTGGTCTGGA
Os_ODD33-pET-f	tgtactttcaaggtgctATGGGTTCTGACTTCAAGGC
Os_ODD33-pET-r	ggtggtgctcgagtgccaTTACATGACGAAGTTTGTCAAG
Gm_2-ODD-C23-pET-f	tgtactttcaaggtgctATGGCAACGGACTTTAGTTC
Gm_2-ODD-C23-pET-r	ggtggtgctcgagtgccaTTACAAATCAACAAAATTTGTGAGGACC
Ava_5009-pET-f	tgtactttcaaggtgcATGACAGTCTTACAACTTCCT
Ava_5009-pET-r	ggtggtgctcgagtgcctCTAAAGCACTTTTTGACG
ALDH7B4-pET-f	tgtactttcaaggtgctgctATGGGTTCGGCGAACAACGAG
ALDH7B4-pET-r	ggtggtgctcgagtgcCTAACCGAAGTTAATTCCTTGC
For Genotyping of T-DNA insertion lines	
Din11-f	TCAAGGGATTTGGATCACTCAC
Din11-r	TCGATCGAATGCATGCATCAC
At3g46930-f	CTGCTGGATACAGGTTTATTCCAC
At3g46930-r	CACGACAATACCCATTAGGCTC
At3g49630-f2	GCTTGAGTGATGTTTCCAAGTAG
At3g49630-r2	GAGGGATGGCAAAATCGTAG
At3g50210-f	CACCATGGCGACGGACTTCAAGTCT
At3g50210-r	AGGTTGGCCATTTGTGAACTCAG
SALK-LB	TTCGGAACCACCATCAAACAG
GABI-LB	AATAACGCTGCGGACATCTAC
SAIL-LB	TACCAATACATTACACTAGCATCTG
For generation and detection of genome editing sites	
gRNA-f	attgCAGATTGGTCATGGAATAT
gRNA-r	aaacATATTCCATGACCAATCTG
Din11-HRM-f	CTGATTATGGTTGGTGAGTGTG
Din11-HRM-r	CAACGATCGTTGATATAGCAGGT
At3g49630-HRM-f	TTGATTTTGGTCGGTGATTGTT
At3g49630-HRM-r	AGCCATCTAATCTAACTAATCGTGA

Lower case letters indicate overlaps with vector sequences for cloning

SI References

Alonso, J. M., Stepanova, A. N., Leisse, T. J., Kim, C. J., Chen, H., Shinn, P., Stevenson, D. K., Zimmerman, J., Barajas, P., Cheuk, R., Gadrinab, C., Heller, C., Jeske, A., Koesema, E., Meyers, C. C., Parker, H., Prednis, L., Ansari, Y., Choy, N., . . . Ecker, J. R. (2003). Genome-wide insertional mutagenesis of *Arabidopsis thaliana*. *Science*, *301*(5633), 653-657. https://doi.org/10.1126/science.1086391

Kleinboelting, N., Huep, G., Kloetgen, A., Viehoever, P., & Weisshaar, B. (2012). GABI-Kat SimpleSearch: new features of the *Arabidopsis thaliana* T-DNA mutant database. *Nucleic Acids Research*, *40*(Database issue), D1211-1215. https://doi.org/10.1093/nar/gkr1047

Sessions, A., Burke, E., Presting, G., Aux, G., McElver, J., Patton, D., Dietrich, B., Ho, P., Bacwaden, J., Ko, C., Clarke, J. D., Cotton, D., Bullis, D., Snell, J., Miguel, T., Hutchison, D., Kimmerly, B., Mitzel, T., Katagiri, F., . . . Goff, S. A. (2002). A high-throughput Arabidopsis reverse genetics system. *Plant Cell*, *14*(12), 2985-2994. https://doi.org/10.1105/tpc.004630

Zhang, H., Zhang, F., Yu, Y., Feng, L., Jia, J., Liu, B., Li, B., Guo, H., & Zhai, J. (2020). A comprehensive online database for exploring 20,000 public Arabidopsis RNA-Seq libraries. *Molecular Plant*, *13*(9), 1231-1233. https://doi.org/10.1016/j.molp.2020.08.001